FLUID PHYSICS BRANCH

RESEARCH DIVISION

OFFICE OF ADVANCED RESEARCH AND TECHNOLOGY

FIFTH INTERCENTER AND CONTRACTORS CONFERENCE ON PLASMA PHYSICS

Part III NASA Lewis Research Center

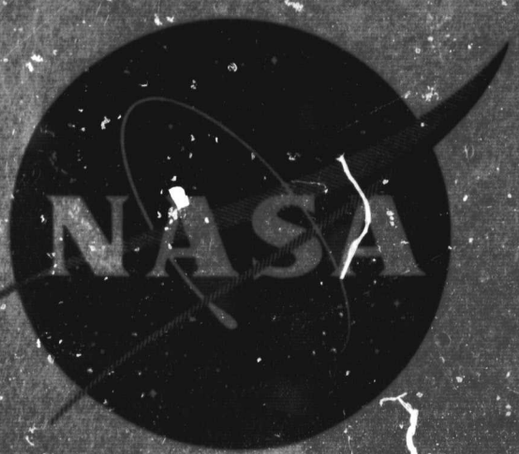

WASHINGTON, D. C.

MAY 24 – 26, 1966

FIFTH NASA INTERCENTER AND CONTRACTORS CONFERENCE ON PLASMA PHYSICS

Part III: Plasma Physics Research at NASA Lewis Research Center

Washington, D. C.
May 24 - 26, 1966

Table of Contents

GENERATING A HOT-ION, MAGNETICALLY CONFINED PLASMA WITH A MODIFIED PENNING DISCHARGE

By J. Reece Roth

Lewis Research Center
National Aeronautics and Space Administration
Cleveland, Ohio

This paper describes a modification of the conventional Penning discharge[1], which is useful in generating large volume, steady-state plasmas, of a type useful in plasma physics and controlled nuclear fusion research. The novel features of this discharge include injection of the operating gas through holes in the anode ring, which allows the discharge to operate in the high-power mode at much lower neutral background gas pressures than is customary with the conventional Penning discharge; operation in strong magnetic fields, up to 20 kG; and placement of the anode ring at the midplane of a magnetic bottle geometry, which makes possible ion trapping and higher ion densities in the magnetic bottle than is possible with the uniform magnetic field conventionally used. This discharge is easy to set up, is repeatable in operation, and can be used as a means of creating a plasma in a magnetic bottle or a minimum-B magnetic field geometry.

A schematic diagram of the discharge is shown in Fig. 1. The anode is operated at a positive potential between 400 and 5000 V dc. The anode is a circular hoop located at the midplane of an axisymmetric magnetic bottle configuration. The grounded superconducting magnet dewars[2], located at the magnetic field maxima, form the cathodes of the discharge. The walls of the vacuum tank are at ground potential. The anode ring and the magnet dewars have a diameter of 18 cm. The axial distance from the anode ring to the cathodes is 10 cm.

The gas required for operation of the discharge is admitted to the vacuum system through a needle valve and enters a 2-liter plenum chamber, which is maintained at pressures from 1 to 5 Torr. The gas inlet line from the plenum chamber is connected to the hollow stainless steel tubing of which the anode ring is constructed. The details of the anode ring are shown in Fig. 2. The hollow interior of the anode ring serves as a manifold to distribute the incoming gas to 3 holes 0.12 cm in diameter, which spray the gas radially inward to the discharge. Conventional Penning discharges are operated at relatively high background pressures of 10^{-3} Torr in the high-power mode of operation. The neutral gas pressure on the axis of this discharge is no more than 5×10^{-5} Torr at a gas flow rate adequate to sustain the discharge in both the low- and the high-power modes of operation. These low pressures are desirable, since ions are then much less

likely to be scattered out of the discharge region by collisions with neutral gas atoms. The characteristic e-folding decay time of the plasma density was measured after switching off the anode voltage. This decay time was typically 7 msec in the low-power mode, and 0.2 msec in the high-power mode of operation.

The conventional Penning discharge is operated with a uniform magnetic field along its axis. In such a magnetic field, ions are accelerated out of the discharge by electric fields existing between the anode and the cathode. This characteristic has permitted a suitably modified Penning discharge to be used as an ion source[3]. In the present geometry, the magnetic mirrors on either side of the anode provide magnetic forces which oppose the electric forces and act to trap ions in the discharge. Preliminary measurements show that the charged particle density on the axis is an order of magnitude higher near the plane of the anode than at the point of maximum magnetic field. The neutral particle density varies by less than a factor of 2 at the same locations. The discharge has been operated at steady-state magnetic field strengths of B_{max} = 4.0, 8.0, 12.0, 16.0, and 20.0 kG, at mirror ratios of B_{min}/B_{max} = 0.55 and 0.39. The discharge characteristics depend only weakly on the magnetic field strength above B_{max} = 4.0 kG. The operation of a Penning discharge in a magnetic-bottle geometry was independently arrived at by Angerth, et al.[4], who reported data from transient operation of their discharge.

It was found that the discharge operates in two distinct modes: a "low-power" mode, in which anode voltages of 500 to 5000 V and anode currents of 0.5 to 50 mA are observed, and a "high-power" mode, in which anode voltages of 500 to 3000 V and anode currents of 0.3 to 9.5 A are observed. As much as 18,000 W has been dissipated in the discharge, and this power dissipation has been limited only by the characteristics of the available power supply. It was found necessary to cool the anode ring with water and the magnet Dewars with liquid nitrogen at discharge levels above 500 W. These cooling provisions are not shown in Fig. 2. Both neon and helium gas were used.

Severe arcing between the anode and one or both cathodes is always observed upon initiating the high-power mode of operation, and has made necessary the inclusion of a ballast resistor in the anode circuit. The discharge has been operated with neon gas in the steady state for 35 min at a constant anode current of 2 A, and a power input of 1900 W. Microwave measurements of a neon plasma at an anode current of 6 A yielded a charged particle density at the midplane on the axis of approximately 5×10^{12} electrons/cm^3. Measurements of ion energy made with a multi-grid probe located outside one of the magnetic mirrors yielded a positive plasma potential of 400 volts and an ion kinetic temperature of an additional 200-400 eV. A neon plasma in the low-power mode of operation had an electron kinetic temperature of 150 eV and a density of approximately 5×10^9 electrons/cm^3, based on the

transition and electron saturation regions of a Langmuir probe uncorrected for the presence of a 5kG magnetic field. The multi-grid probe revealed low-power mode ion kinetic temperatures of up to 2500 eV. Some preliminary data on plasma turbulence frequency spectra will be presented at the meeting.

References

1. F. M. Penning, and K. Nienhuis, Phillips Tech. Rev., 11, no. 4, 116 (1949).
2. J. R. Roth, D. C. Freeman, Jr., and D. A. Haid, Rev. Sci. Instr., 36, 1481 (1965).
3. R. G. Meyerand, Jr., and S. C. Brown, Rev. Sci. Instr., 30, 110 (1959).
4. B. Angerth, J. Ehrensvard, and H. Persson, Paper no. CN 21/5, Presented at 2nd Conf. on Plasma Physics and Controlled Nuclear Fusion Research, Culham (England), Sept. 6-10, 1965.

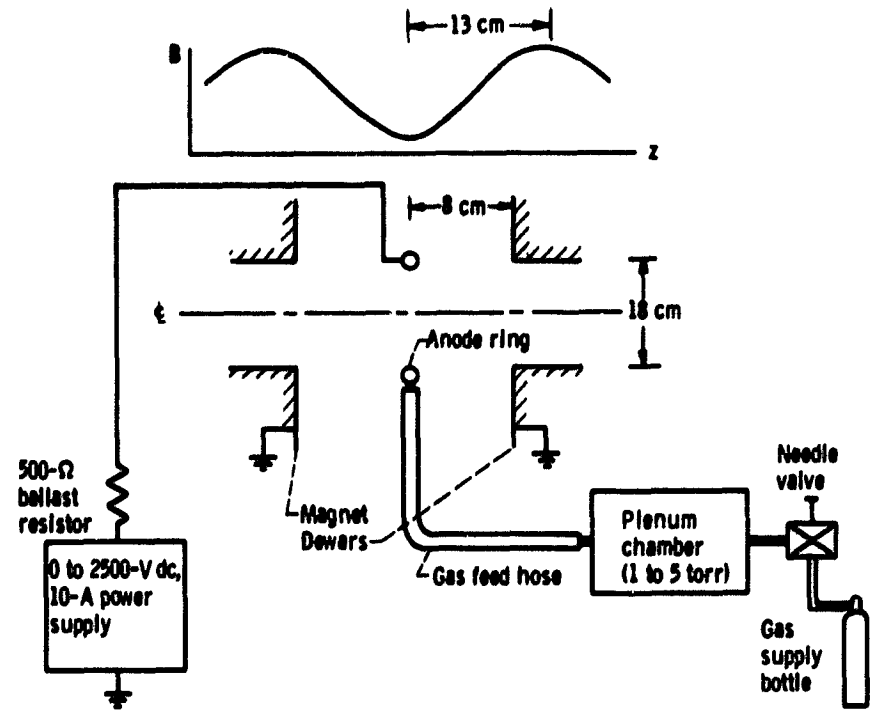

Figure 1. - Electrical and gas flow systems.

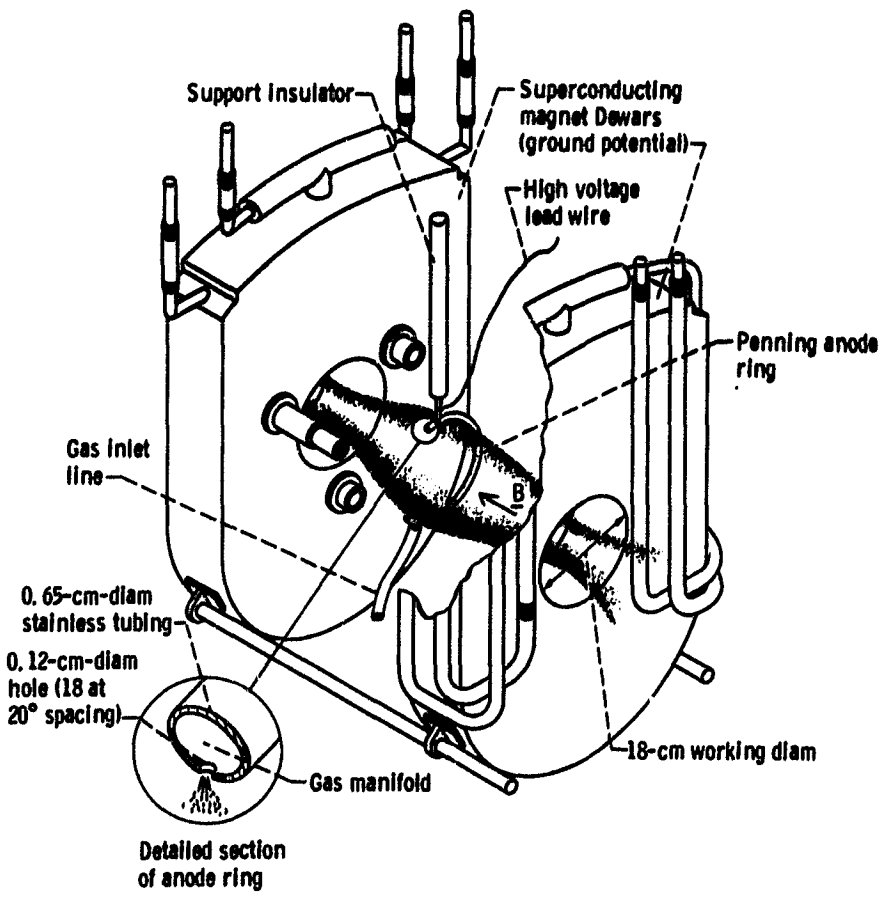

Figure 2. - Discharge operating configuration and detail of anode ring.

HARMONIC RESPONSE OF FORCED NON-LINEAR PLASMA WAVES

By Richard R. Woollett

Lewis Research Center
National Aeronautics and Space Administration
Cleveland, Ohio

Linear approximations are more frequently used than not in defining small amplitude plasma wave motion. However, the resulting linearized equations are often used without reservation in problems where the magnitude of the wave amplitude may be sizable. With experiments being conducted in plasma heating where energy addition is via large amplitude waves and with experiments being conducted near or at resonances which usually tax the credibility of any simple model, the evaluation of the linear approximation is paramount.

The starting point for a wave analysis is generally Ohms law and the equation of motion of a fluid element (or equation of motion of the species). If the non-linear terms are retained, the expressions are difficult to solve. To make the problem tractable, investigators utilize various assumptions. One such heuristic hypothesis entails assuming a specific structure for the non-linear wave. Experimental characteristics can be used as a guide to establish the a priori structure. One typical characteristic of experimental non-linear steady state systems is that numerous harmonics are present in addition to the fundamental forcing frequency. If the linear and assumed infinite set of non-linear waves are planer and if all are propagating in a given direction, the a priori structure of the non-linear wave can be written as

$$\bar{A} = \sum_{j=1}^{\infty} \bar{A}_j = \sum_{j=1}^{\infty} \tilde{\bar{A}}_j e^{i(k_{xj}x + \omega_j t)}$$

This particular expression will represent the form of all oscillating quantities appearing in the analysis; propagation is assumed to be in the x direction. When the order of magnitude of the ascending coefficients of the series is monotonically decreasing the expressions are well suited for a perturbation technique.

Applying this perturbation expansion of the non-linear waves to the equations of motion, Ohms law, conservation expressions for mass, species and charge and to Faraday's law, one can obtain the perturbations to the particle currents in terms of the amplitudes of the linear components of the electric field.

After substituting these expressions for the currents into the wave equation and equating terms of equal magnitude, there results a set of equations where all variables except the perturbation electric fields are eliminated. This hierarchy of solutions starts with the normal linear solutions. They can be represented in tensor notation by

$$[A_{ij}^{\lambda}][E_j^{\lambda}] = [B_{ij}^{\lambda-1}][(E^{\lambda-1})_j^2]$$

where λ represents the order of perturbation; for $\lambda = 1$, the right hand side vanishes. The left hand side has the identical form as the linear solution regardless of λ. Consequently the electric field of any order of perturbation can be calculated by obtaining the next lower terms.

The technique described above was applied to a uniform density, cold, collisionless plasma, of infinite extent, immersed in a uniform magnetic field. Non-linear wave amplitudes were calculated for the four principal first order plane waves; ordinary and extraordinary waves propagating perpendicular to the magnetic field, and the right and left hand polarized waves propagating parallel to the magnetic field.

Calculations show that for both an ordinary and extraordinary first order wave the second order non-linear disturbance is an extraordinary wave, i.e., it is a function of the magnetic field strength. In all cases the first harmonic has the same phase velocity as the fundamental but twice the frequency. The magnitude of disturbances higher than the second were not examined. For both the ordinary and the right and left circularly polarized fundamental, the linear approximation is satisfactory even for large amplitude linear components. This is not the case for the extraordinary fundamental. The amplitude ratio of the extraordinary fundamental is plotted in the figure for densities of 10^{11}, 10^{12}, and 10^{14} cm^{-3}. The amplitude ratio is the quotient of the amplitude of the non-linear wave to the square of the amplitude of the linear wave. There are four singularities present. The range of influence of all but the first is limited to rather restricted frequency regions. At frequencies below the first singularity, the amplitude ratio of the first harmonic wave is fairly constant and increases as the density increases. Decreasing the magnetic field intensity will shift the first singular point to lower frequencies. Concomitantly the amplitude ratio for frequencies less than the first singularity increases significantly

as the magnetic field decreases. The first singularity (when at low frequencies) occurs at the Alfven velocity. For an atomic hydrogen plasma and for the range of densities and field strengths investigated, this occurs around 0.2 of the ion cyclotron frequency.

To obtain the ratio of the amplitude of the first harmonic to that of the fundamental, multiply the amplitude ratio by the amplitude of the linear wave in stat-volts/cm. Consequently for a fundamental of 1 stat-volt/cm, the linearity approximation is probably invalid over the regions marked by the double curve. Although 1 stat-volt/cm is a rather large wave amplitude, such values do exist in high power experiments. One-tenth of this electric field certainly is not unreasonable though. At these latter conditions for densities of 10^{12} cm^{-3} and greater, there exist extended regions where the linearity approximate is invalid.

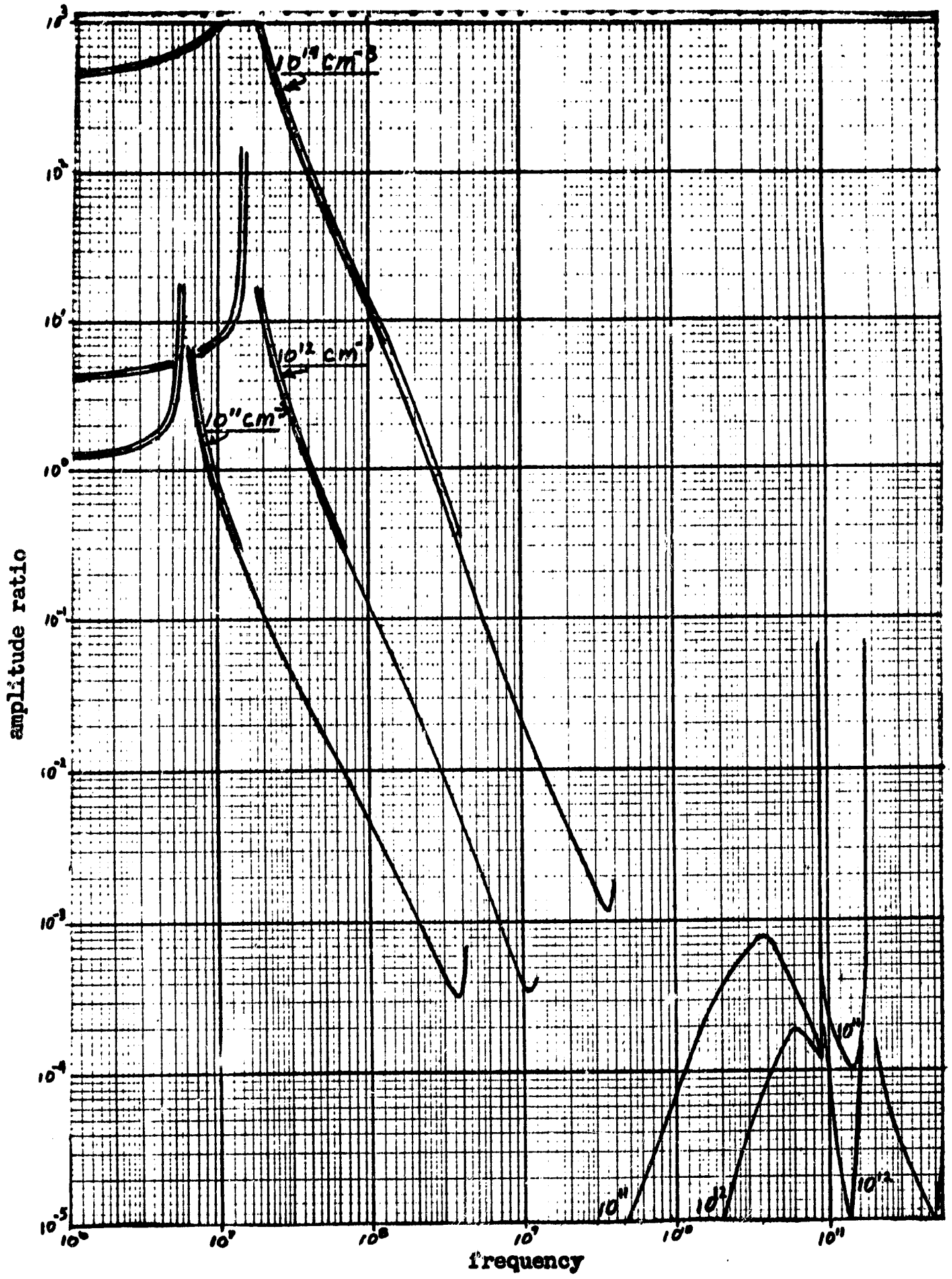
10^{13}
10^{12} cm^{-3}
10^{11}
10^{10}
10^{9}
10^{8}
10^{7}
10^{6}
10^{5}
10^{4}
10^{3}
10^{2}
10^{1}
10^{0}
10^{-1}
10^{-2}
10^{-3}
10^{-4}
10^{-5}
10^{6}
10^{7}
10^{8}
10^{9}
10^{10}
10^{11}
10^{12}
10^{13}
amplitude ratio
frequency

R. F. POWER TRANSFER TO ION-CYCLOTRON WAVES

By D. R. Sigman and J. J. Reinmann

National Aeronautics and Space Administration
Lewis Research Center
Cleveland, Ohio

ABSTRACT

The generation of ion-cyclotron waves in a plasma column is of interest to experimentalists concerned with the heating of plasma through collisionless processes. One method for transferring power to these waves is to wrap a current sheet around the plasma column. The current sheet has an azimuthal current density varying axially as $e^{ik_0 z}$ and is two wavelengths long. Equations have been derived and calculations made from a theoretical plasma model of the effect of various plasma parameters on the power transferred from the current sheet to ion-cyclotron waves in the plasma. The analysis includes electron inertia terms and radial density variations which were not included in previous work.

It was found that the inclusion of electron inertia terms reduces power transfer. Optimum coil wavelengths and optimum electron densities have been calculated for several plasma configurations. For typical plasmas, the optimum density for power transfer is between 1×10^{12} cm^{-3} and 5×10^{12} cm^{-3}. Figure 1 shows peak power transfer versus electron density for a 5 cm radius plasma. The current sheet had a wavelength of 45 cm and a 10 cm radius.

Figure 2 shows the radial density distributions which were studied. In general, power transfer to inhomogeneous plasmas is large when the volume average density is near the optimum density computed for homogeneous plasmas.

Figure 3 shows a typical resonance absorption curve. The half-width is determined primarily by the value of Ω for which peak power occurs. For low densities ($n_e < 5 \times 10^{12}$ cm^{-3}), and near the peak power point, r. f. power is coupled predominantly to a single plasma mode of oscillation. At high densities and at off-resonance points for low densities the power may be distributed among several modes with different axial wavelengths, thus making it difficult to measure plasma wave properties at off-resonance conditions.

Figure 1

Relative Power Transfer vs. Electron Density

plasma radius = 5 cm.
coil radius = 10 cm.
coil wavelength = 45 cm.

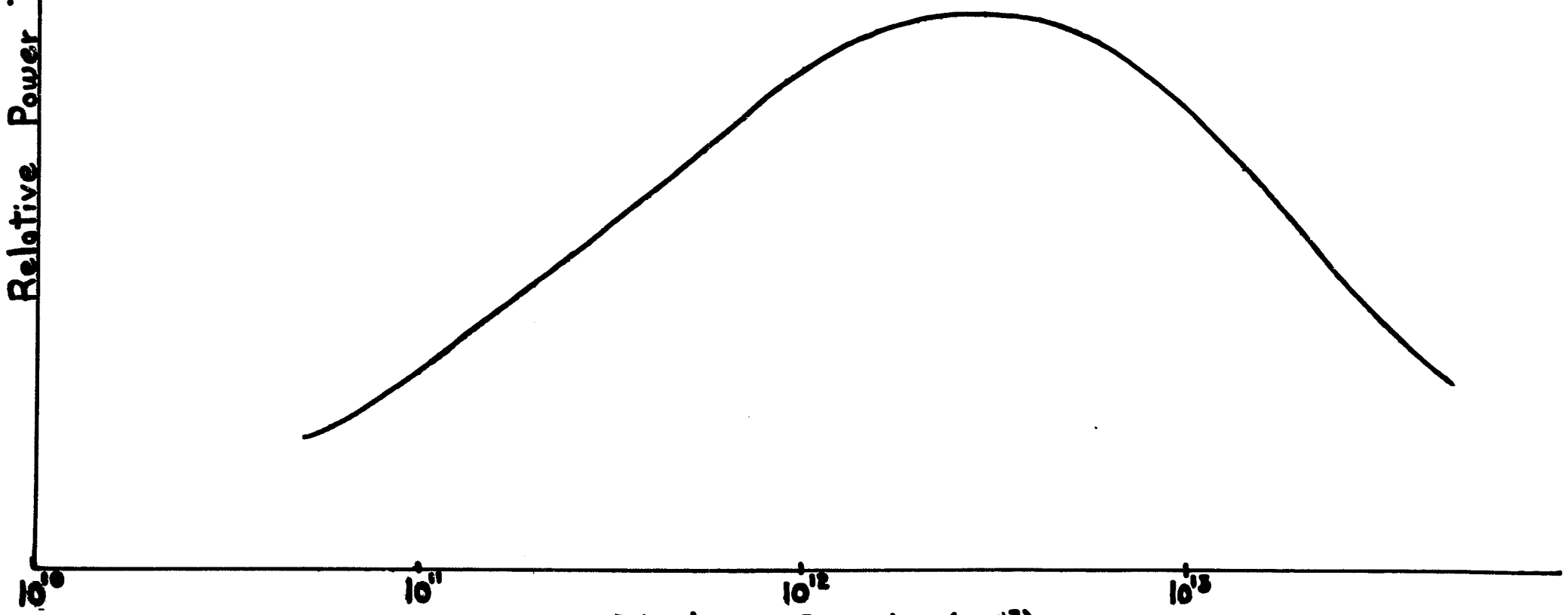

Figure 2
Electron Density Variations

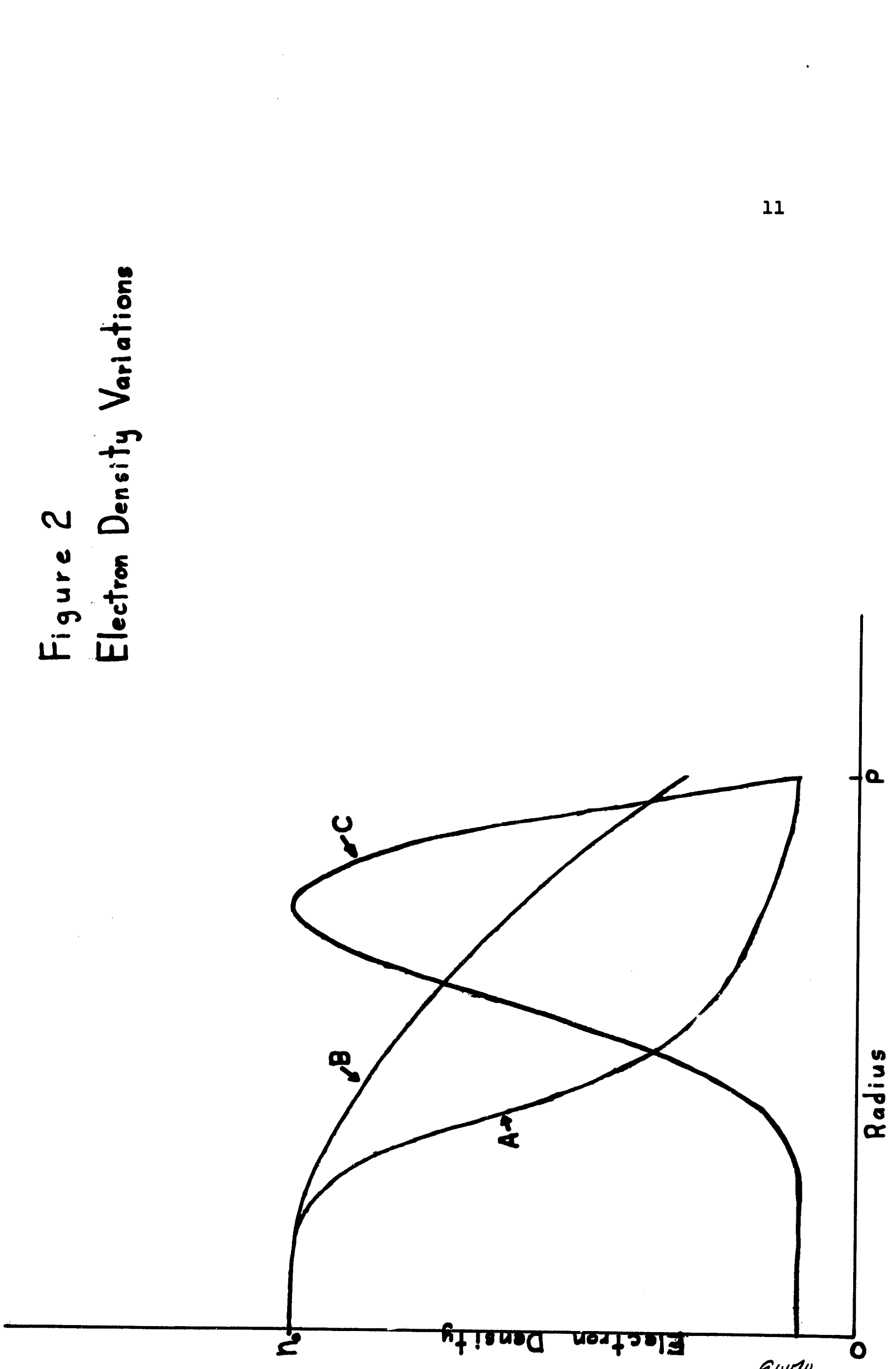

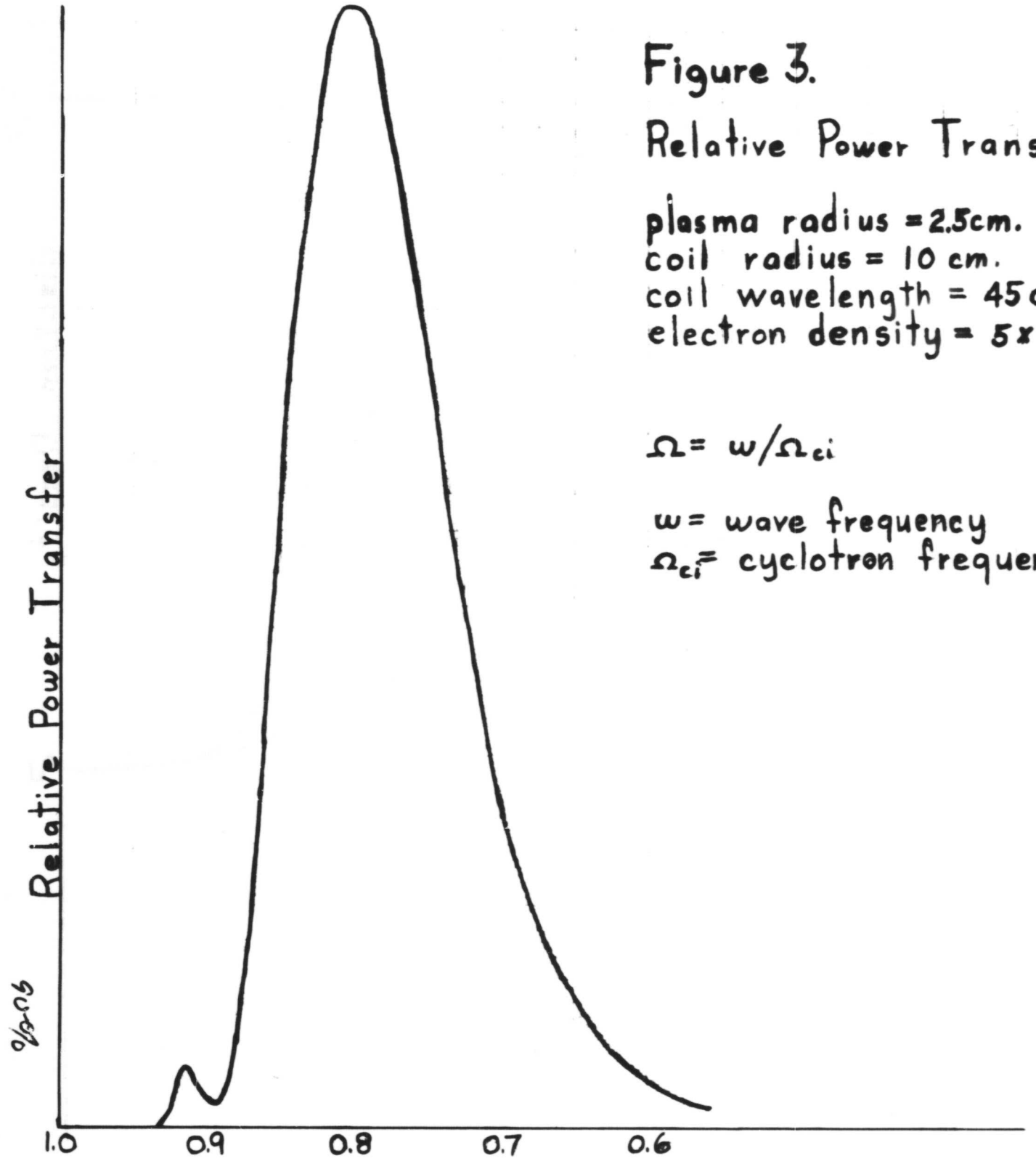

Figure 3.

Relative Power Transfer vs. Magnetic Field

plasma radius = 2.5cm.
coil radius = 10 cm.
coil wavelength = 45cm.
electron density = 5×10^{12} cm^{-3}

$\Omega = \omega / \Omega_{ci}$

ω = wave frequency
Ω_{ci} = cyclotron frequency

ELECTRON IMPACT CROSS SECTIONS FOR ATOMIC AND HYDROGEN CALCULATED BY GRYZINSKI'S CLASSICAL THEORY

By George M. Prok, Carl F. Monnin and Henry J. Hettel

National Aeronautics and Space Administration
Lewis Research Center
Cleveland, Ohio

ABSTRACT

In plasma experiments, a knowledge of the energy loss mechanisms is important. A major loss mechanism is the radiation produced by inelastic collisions of electrons with molecules or atoms. Detailed knowledge of the cross sections involved is necessary to predict the magnitude of this radiation loss.

Excitation and ionization cross sections for electron scattering in ground state and metastable atomic hydrogen were calculated by the Born approximation and by the classical theory of Gryzinski. The classical theory leads to two excitation cross sections depending on whether a velocity distribution or an average value was assumed for the velocity of the atomic electron. Gryzinski also developed an exchange formula which was used for s→s transitions in atomic hydrogen. Sample curves are presented for exchange and excitation of atomic hydrogen in figures 1 and 2 respectively.

A model for applying Gryzinski's classical theory to diatomic molecules is also presented. Since Gryzinski's theory is one of Coulomb interaction, the variation of electron energy as the molecule vibrates must be known for each electronic state in order to apply this classical theory to a diatomic molecule. The electron energy as a function of internuclear separation for the various electronic states can be described by a Morse potential curve. The energy relation between the Morse curve for the ground state and the Morse curve for any excited state of a diatomic molecule, such as H_2, is shown schematically in figure 3.

According to the Franck-Condon principle, electronic excitation takes place at a constant r because this process is much more rapid than the molecular vibrational motion. This means that, at any given instant of time for an internuclear separation r, an energy of $T_0(r-r_e)_u$ is required to electronically excite state u. From figure 3 it can be seen that for any given electronic excitation the value of $T_0(r-r_e)_u$ will vary with the internuclear separation. Because of this variation, application of Gryzinski's theory can only be applied to a constant r. The probability that the internuclear separation is a given value of r can be determined from the probability density distribution of a harmonic oscillator. Thus a weighting factor

is determined to be applied to Gryzinski's cross section at a constant r. The products of the weighting factors and the cross sections for number of r's are summed to give the cross section for the electronic transition.

This model was used to calculate the excitation cross section and exchange cross section for the individual excited states of molecular hydrogen from its ground state. Theoretical cross sections are presented for both the singlet and triplet systems. The energy range is from onset to 360 ev. The ionization cross section is compared with absolute experimental data and is found to agree in the energy range considered.

FIG. 1

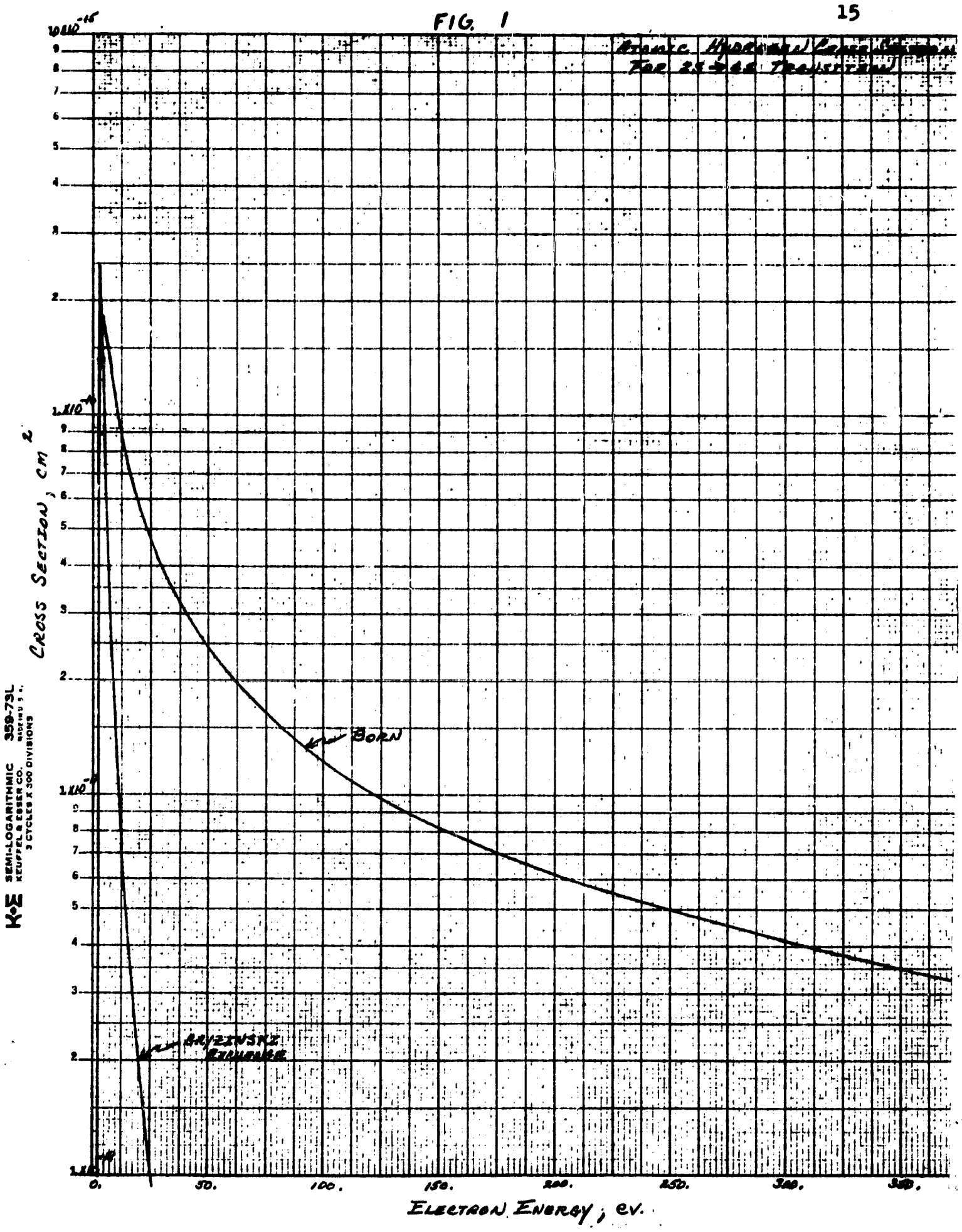
Cross Section, cm²
Electron Energy, ev.
Born
Brysinski
0.
50.
100.
150.
200.
250.
300.
350.

K·E SEMI-LOGARITHMIC 359-64
KEUFFEL & ESSER CO.
2 CYCLES X 100 DIVISIONS

FIG. 2

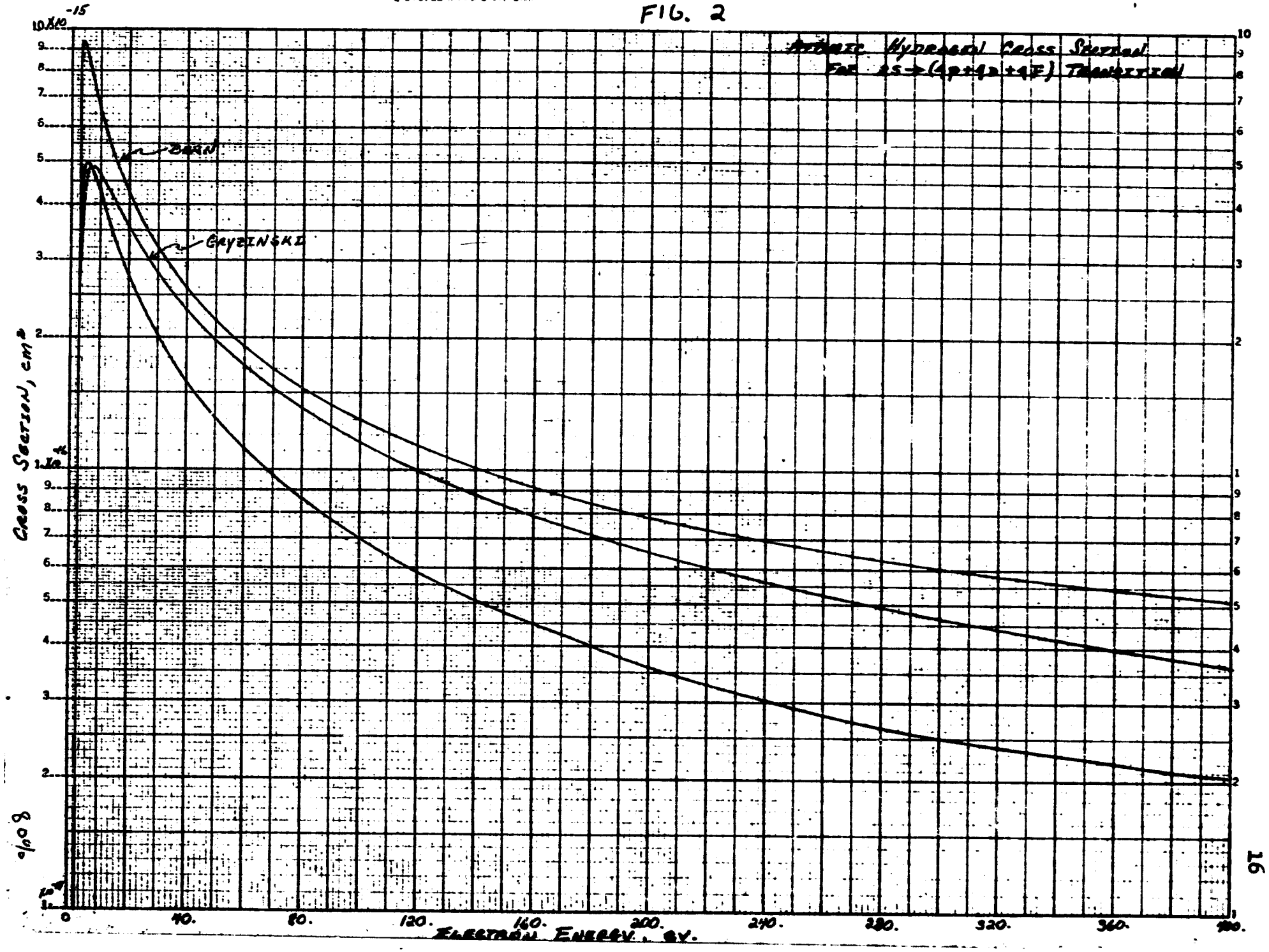

FIG. 3

MODEL FOR CALCULATING ENERGIES INVOLVED IN EXCITING DIATOMIC MOLECULES

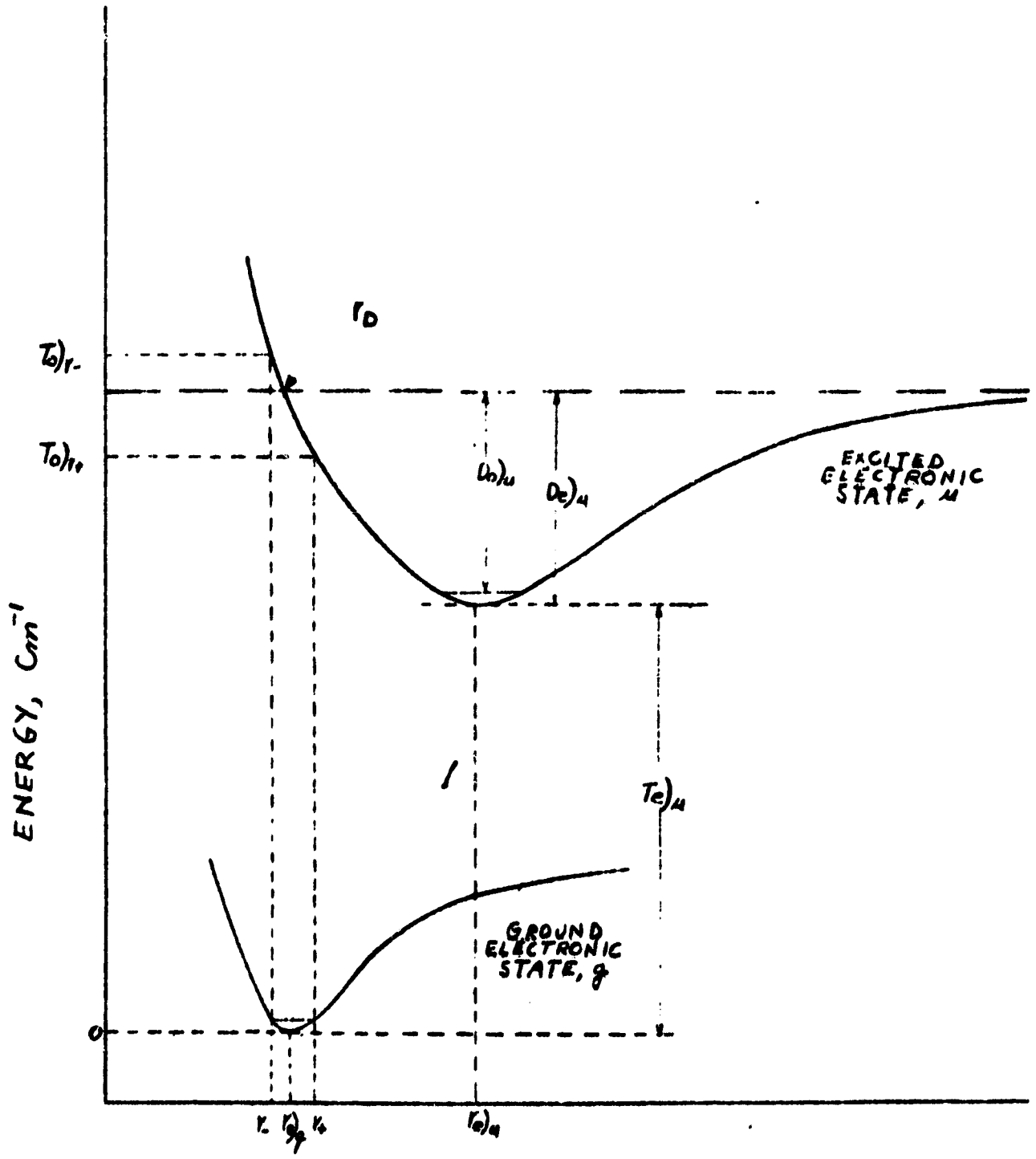

PRELIMINARY MEASUREMENTS OF PLASMA FLUCTUATIONS IN A HALL CURRENT ACCELERATOR

By John S. Serafini

National Aeronautics and Space Administration
Lewis Research Center
Cleveland, Ohio

ABSTRACT

The present investigation is a preliminary attack on the problem of spontaneously occurring plasma oscillations and/or plasma fluctuations which have been noted to exist in steady-state plasma devices. The initial plasma device chosen was an annular Hall-current plasma accelerator utilizing a radial magnetic field and a slightly-ionized low-current argon discharge. The ultimate goal is to ascertain the role of plasma fluctuations in determining the characteristics of the bulk plasma behavior.

The approach used is similar to those used in fluid-dynamic turbulence investigations in which the mean-square, the frequency spectra, and the space-time correlations of the spectra are measured. The present research is directed toward plasma fluctuations which are concentrated at the low end of the frequency spectrum to minimize the difficulties with the diagnostics.

The initial measurements of the fluctuations are being made using electrostatic probes at various conditions of probe bias voltage. In addition to measurements of the r.m.s. magnitude, the amplitude spectra of the fluctuations have been measured from 100 cps to 600 kc. Space-time correlations of the fluctuations have been made with a correlation analyzer having a response up to 500 kc. The coherence of the fluctuations along the axial and lateral directions has been measured. The fluctuations possess a significant coherence in the longitudinal direction for the length of the accelerator. Similar coherence exists in the lateral direction. No convective effects of the fluctuations have been observed.

The present and future research is being devoted to extending and analyzing the previously obtained results. Measurements to be made include the use of magnetic and emissive probes as sensors of the plasma fluctuations.

NASA
CS-37702

HALL CURRENT ION ACCELERATOR

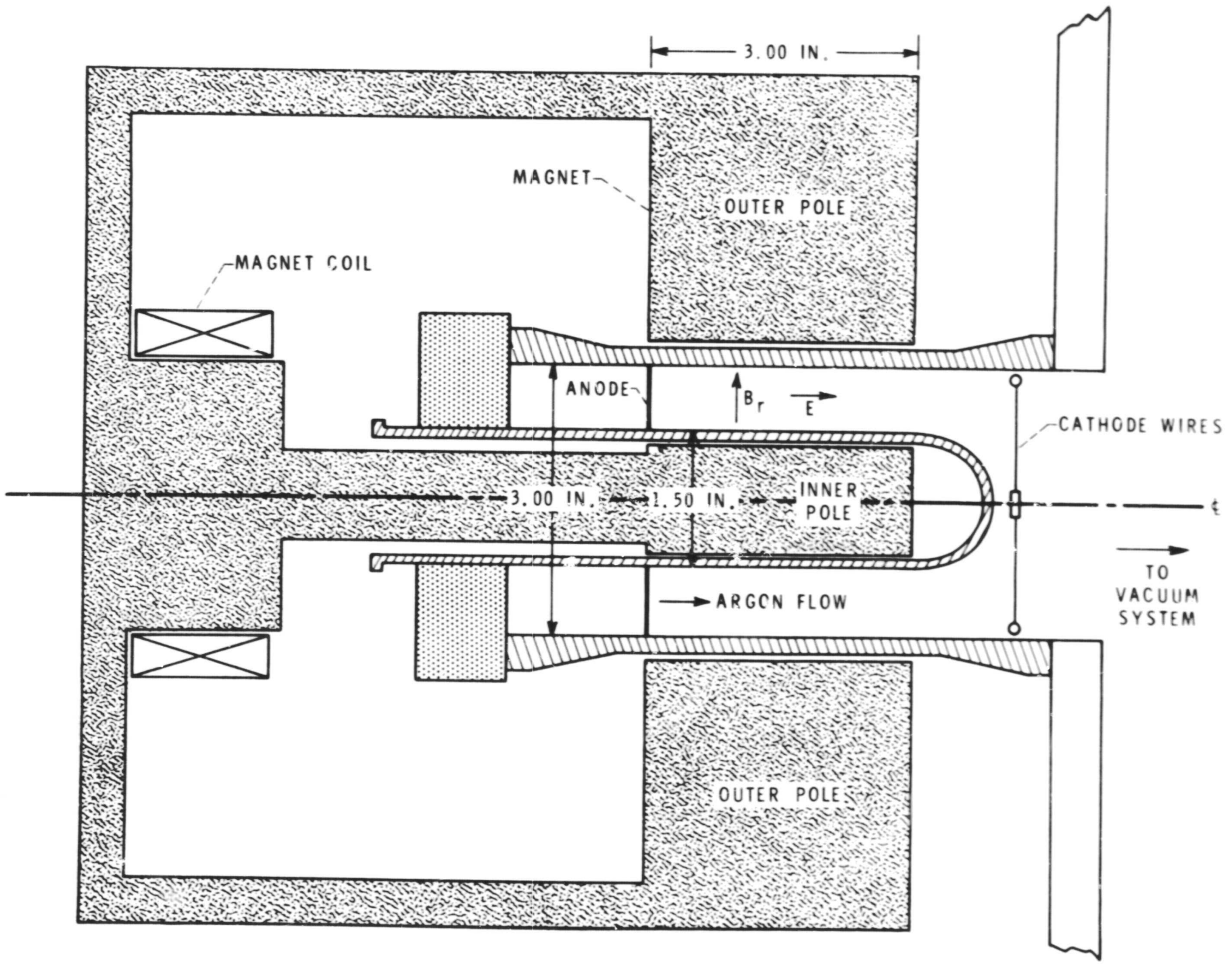

TYPICAL SPECTRA FOR CORRELATION MEASUREMENTS

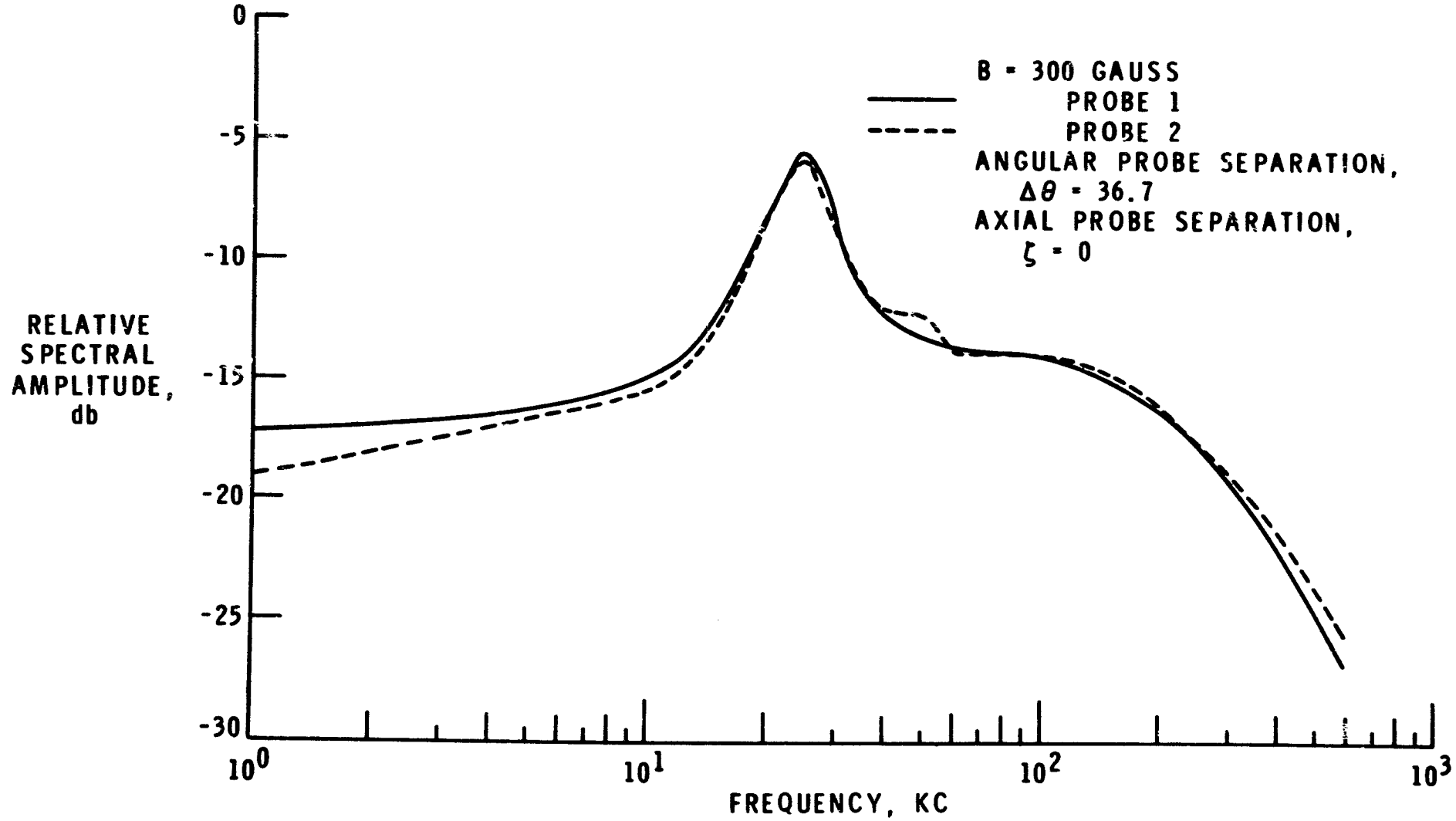

CORRELATION COEFFICIENT VS TIME DELAY

B = 300 GAUSS

$$\text{CORRELATION COEFF, } R(\tau) = \frac{\overline{e_1(t)e_2(t+\tau)}}{\sqrt{\overline{e_1^2(t)}}\sqrt{\overline{e_2^2(t)}}}$$

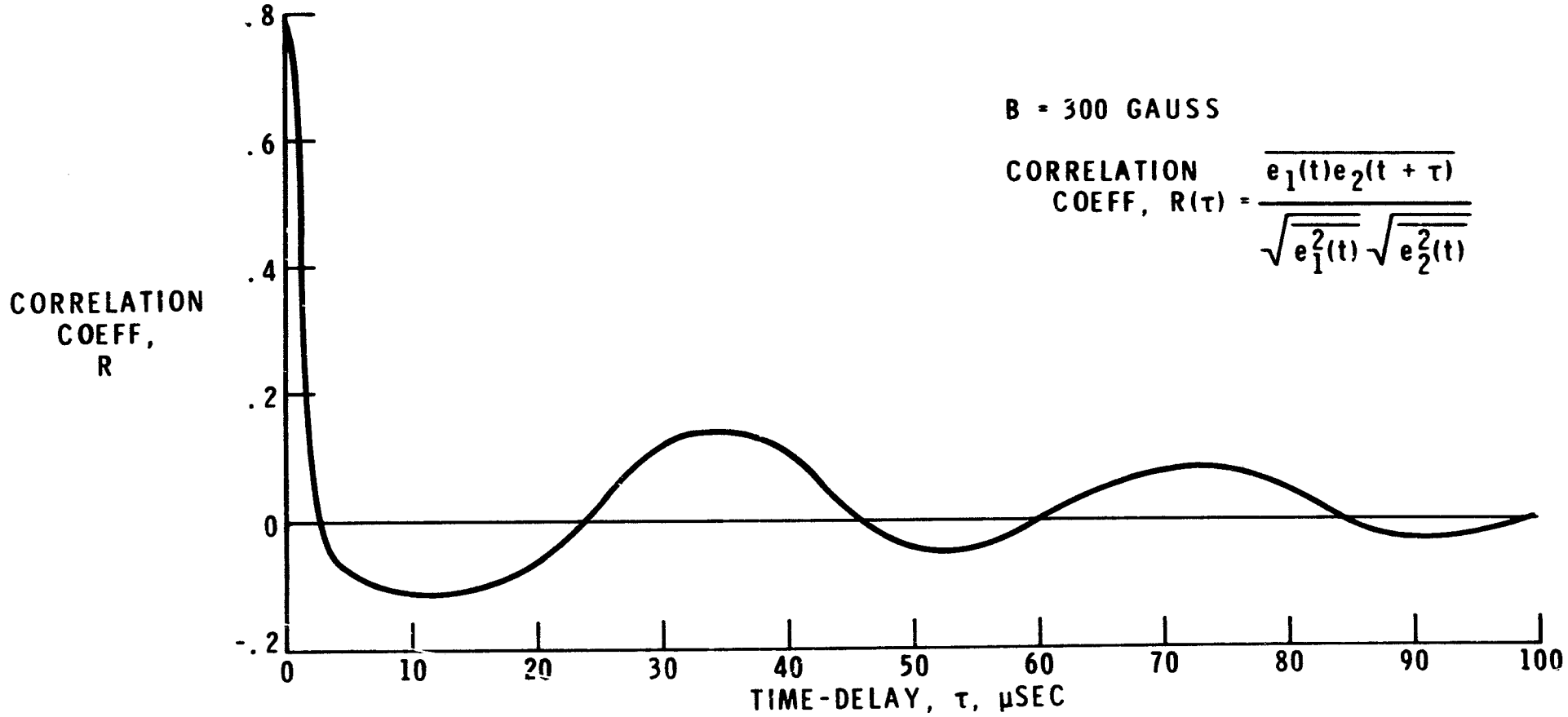

MAXIMUM CORRELATION AS A FUNCTION OF AZIMUTHAL PROBE SEPARATION

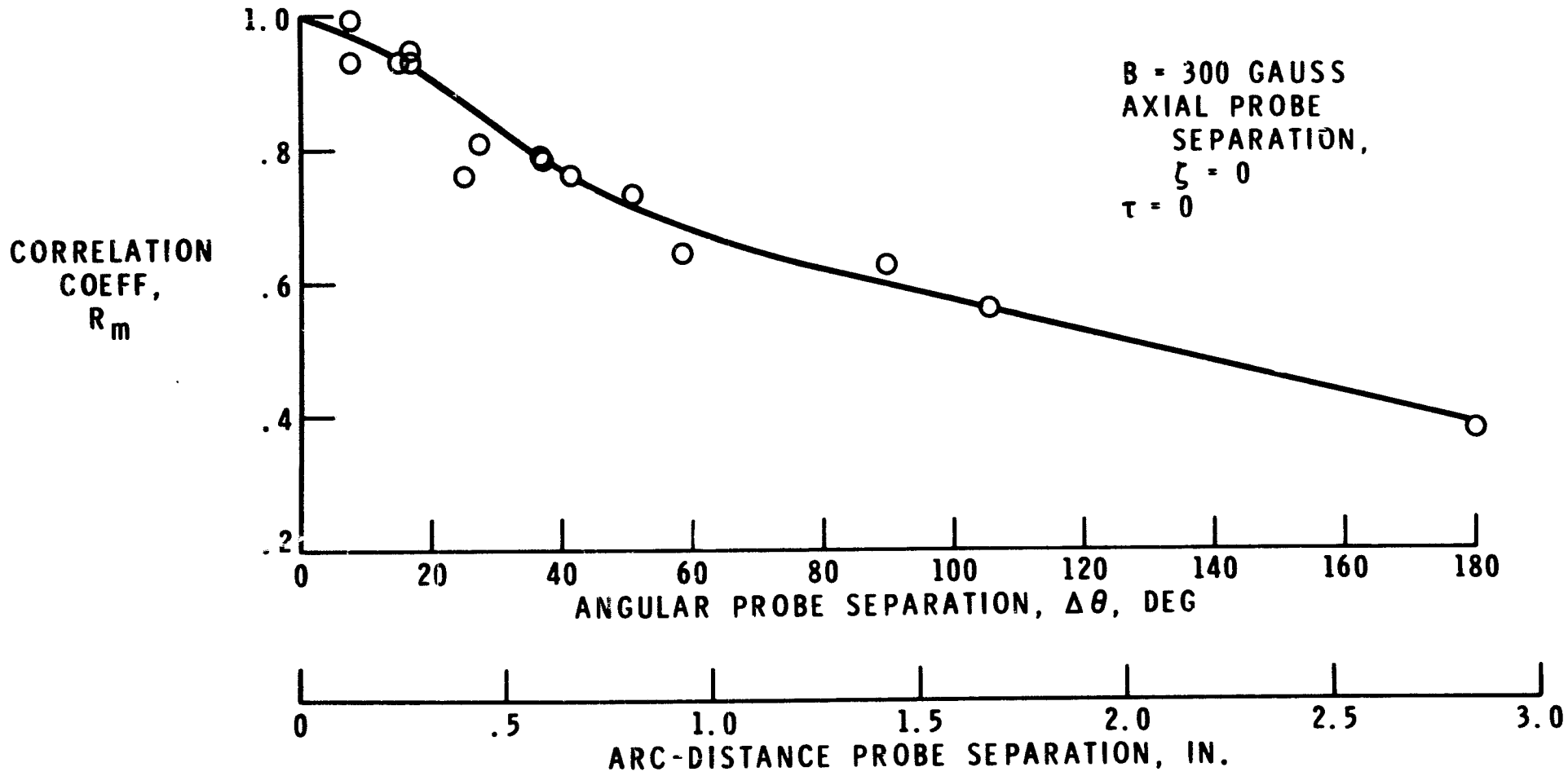

EFFECT OF MAGNETIC BEACH ON R. F. POWER ABSORPTION IN ION CYCLOTRON RESONANCE

By Clyde C. Swett

National Aeronautics and Space Administration
Lewis Research Center
Cleveland, Ohio

ABSTRACT

A brief experimental survey has been undertaken to determine the effect of adding a variable magnetic beach to an apparatus being used to investigate the generation and thermalization of ion cyclotron waves. In this apparatus ion cyclotron waves are generated in a hydrogen-plasma column in a magnetic-mirror geometry by means of an r. f. coil, the initial plasma column being a hot-cathode discharge and the complete system operating steady state. If a magnetic beach - i. e., a region where the magnetic field strength decreases in the direction of wave propagation - is used, the energy in the wave will be transferred to the ions and the ions will be heated to high temperatures. If the beach is inside of the mirrors, such ions might be contained and the plasma density improved.

Adding a beach, however, is a major system change that might result in the need for other modifications in the apparatus. For this reason it was decided to make a quick survey to (1) determine the effect of magnetic beach on r. f. power absorption, (2) determine if the plasma density is increased because of thermalization of the waves, (3) determine if the beach is detrimental to the operation of the hot-cathode discharge, (4) determine if the wavelength of the waves in the beach is decreasing, thereby showing that thermalization is occurring, and (5) observe the effect of the beach on resonances.

Results show that r. f. power absorption decreased about 20 percent when the field at the beach position was reduced to 89 percent of the main field. No increase in plasma density could be observed and only slight effect on the hot-cathode discharge was apparent. Attempts to measure wavelength change in the beach failed because the magnetic-probe signals appeared to be the resultant of at least two waves. Close examination near the theoretical resonant point shows two peaks in the power absorption. The point closest to the theoretical point has been observed both with and without beach, but the peak farthest from the theoretical point has only been observed with the beach present. It is an extremely sharp peak and the half-width of resonance cannot be measured at the present time. Possible causes for the second peak presently being considered include (1) striations in the discharge, (2) reflections of the waves, (3) existence of waves other than the

ones expected, and (4) non-uniformities in the field. Two equipment modifications appear necessary - a more uniform plasma column and a longer magnetic field region for making wavelength measurements.

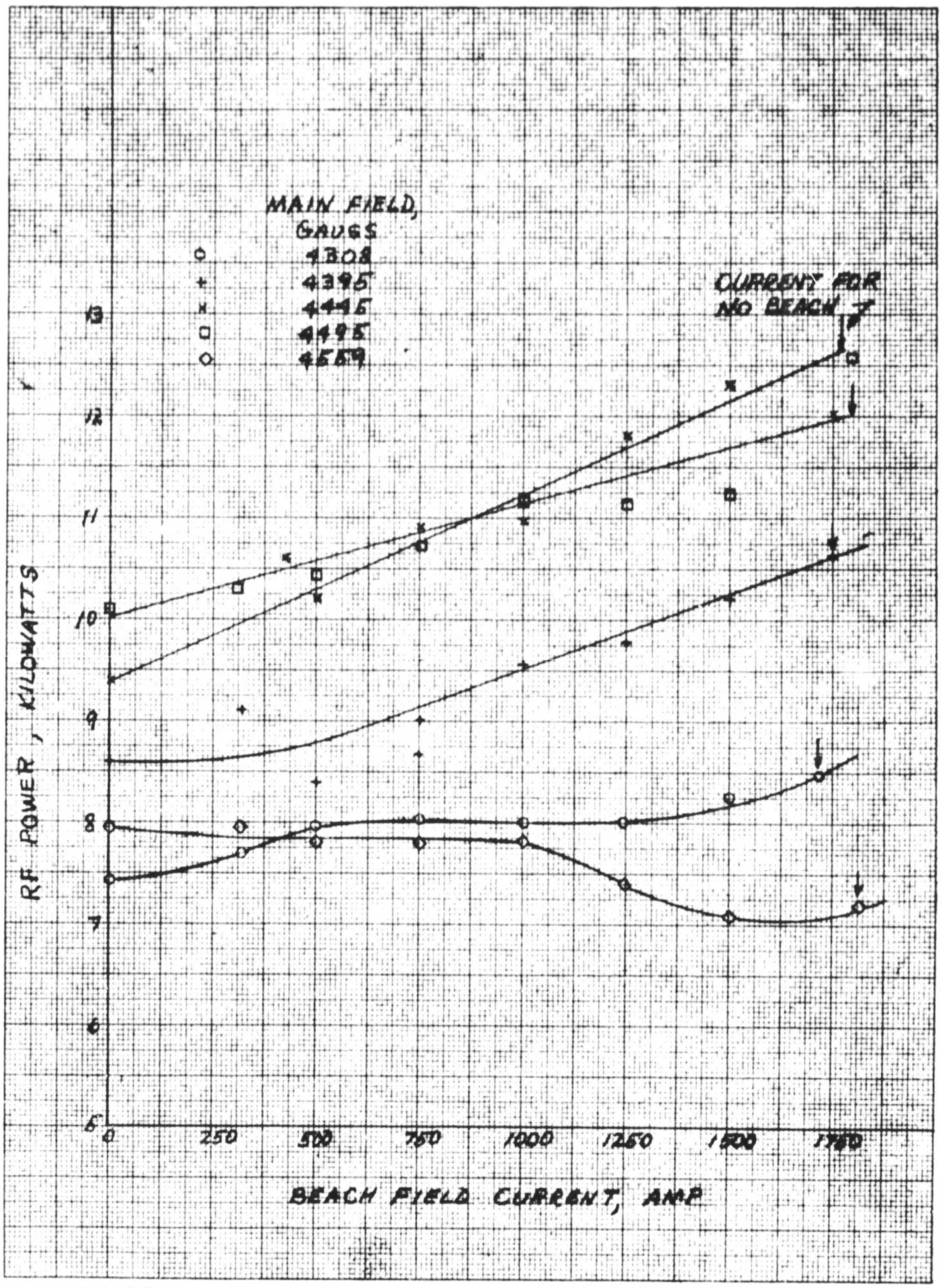

EFFECT OF BEACH ON RF POWER

THE POSSIBILITY OF ANOMALOUS CATHODE EMISSION ASSOCIATED WITH A CURRENT OF LOW ENERGY IONS

By J. E. Heighway

National Aeronautics and Space Administration
Lewis Research Center
Cleveland, Ohio

ABSTRACT

Except in special cases, an ion current impinging upon a cathode results in an electron emission at least sufficient to neutralize the ion current. It would seem possible that such an ion current might produce an electron emission (over and above that required for neutralization) which exceeds the thermionic saturation current. This anomalous emission may occur by virtue of the possibility that the ions, as they approach the cathode surface, lower the local work function and enhance the probability of tunneling. A simplified one-dimensional model, which should afford approximate estimates of this effect, is presented.

CONSIDERATION OF IRREVERSIBLE THERMODYNAMICS AS AN APPROACH TO MHD PLASMA PROBLEMS

By N. Stankiewicz

National Aeronautics and Space Administration
Lewis Research Center
Cleveland, Ohio

ABSTRACT

If it is assumed that the local entropy of a plasma is a function of the various averages over the distribution function, f_j, (j^{th} species), then, a closed form expression for f_j can be obtained. This expression contains undetermined parameters which, in theory, can be determined from the coupled moments of the Boltzmann collision equation. There is, however, no advantage to solving for these parameters in this way, and in fact the collision integrals are somewhat more complicated than they would be in the usual Chapman-Enskog method of solution.

The advantage of this method would seem to be in identifying the entropy production source term which arises due to irreversible processes. This term is a product of the fluxes and the conjugate thermodynamic "forces" operating in the system. (These "forces" are given by taking the gradient of those undetermined parameters contained in the distribution function). From a consideration of this term and the second law of thermodynamics it may be possible to determine limits on the properties of a non-equilibrium process. However, the primary difficulty is to find a rigorous method of identifying the undetermined parameters in terms of the physically applied forces (e.g. those due to electric and magnetic fields) which drive the system into non-equilibrium states.

STATUS OF LARGE VACUUM FACILITY H_2, NH_3, AND Li MPD ARC TESTS

By D.J. Connolly, R.E. Jones, S. Domitz, and G.R. Seikel

National Aeronautics and Space Administration
Lewis Research Center
Cleveland, Ohio

ABSTRACT

Studies of magnetoplasmadynamic (MPD) arc thrustors are presently being conducted in NASA Lewis Research Center's 15-foot-diameter, 65-foot-long vacuum tank. Results to date include performance data for two different thrustor configurations with hydrogen and ammonia propellants and tank pressures from 0.6 to 5×10^{-5} millimeters of mercury. The second of the two configurations has also undergone preliminary tests with hydrogen-lithium mixtures and is presently being tested with pure lithium.

The results for the first of the two configurations are described in reference 1. Subsequent to publication of reference 1, a systematic error was discovered in the ammonia flow rate calibration, all ammonia flow rates being a factor of 2.04 larger than reported. Hence, all specific impulse and thrust efficiency data should be reduced by a factor of 2.04. A corrected specific impulse versus thrust efficiency curve is attached.

Preliminary results for the second configuration - one which was designed to operate on lithium - show poorer hydrogen and ammonia performance than the configuration of reference 1. The lithium thrustor, however, appears to perform well on lithium-hydrogen mixtures.

Future plans include testing of the lithium thrustor at tank pressures down to 2×10^{-6} millimeters of mercury and thorough diagnosis of the thrustor beams with a Langmuir-calorimetric probe array.

Ref. 1: Jones, R.E., Walker, E.L., AIAA Preprint 66-117, 1966.

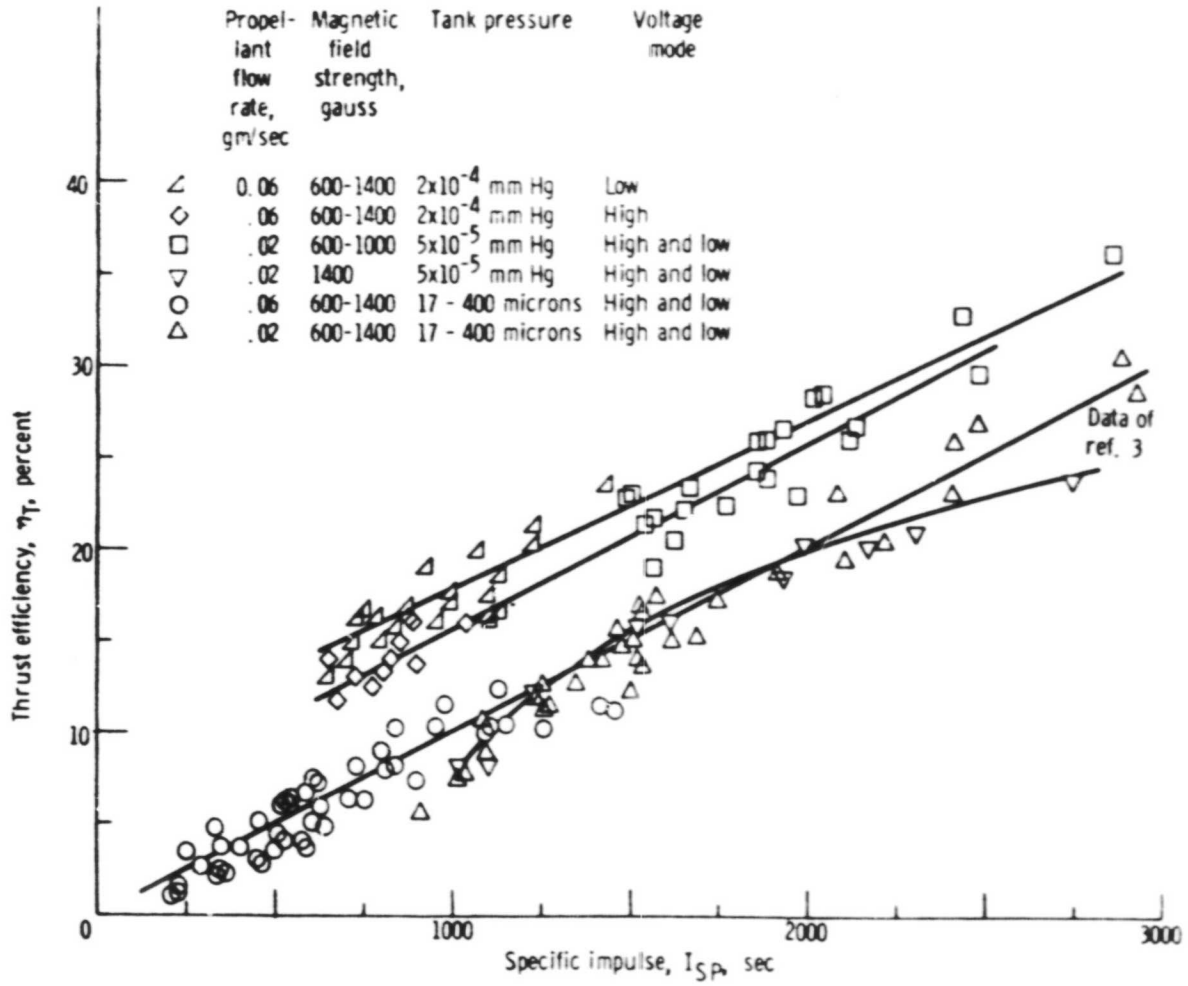

MPD arc thrustor performance (ammonia propellant).

PERFORMANCE, ENDURANCE, AND DIAGNOSTICS OF MAGNETIC EXPANSION THRUSTOR

By D.N. Bowditch and A.E. Johansen

ABSTRACT

A simple, low-power MPD arc, termed a D.C. magnetic expansion thrustor, has been under investigation at NASA Lewis Research Center (reference 1 and 2). An electrical discharge is supported in an axial magnetic field between a cylindrical anode and a hollow cathode centered on the anode axis. The thrustor is operated in a D.C. magnetic field which is typically 250 gauss with Argon propellant at mass flows varying from less than 0.2 mg/sec to more than 0.5 mg/sec. The propellant is injected into the anode through both the hollow cathode and small feed tubes along the anode walls. The discharge characteristics are controlled by the hollow cathode flow and the anode voltage such that the discharge current is generally 2-3 amps while the discharge voltage is maintained over a range of 60-170 volts (150-500 watts). In general, kinetic efficiency improves and specific impulse increases with higher voltage, but thrust/power ratio reaches a maximum usually below 300 watts. The best performance to date has been about 15% kinetic efficiency at a specific impulse of 1800 sec and with a thrust/power ratio of 4 mlb/kw. The performance of various thrustor sizes and coil spacings at varying powers and mass flows is presented along with an evaluation of various hollow cathode sizes and materials. One tantalum cathode with a .044" ID x .014" wall and coated on the inside with a mixture of barium carbonate and carbon ran continuously for over 400 hours before being shut down.

The thrustor operates as a low-pressure thermal expansion device. Since no net current can flow from the thrustor the non-equilibrium plasma establishes an axial electric field which couples the expanding energetic electron gas to the ions. The expansion is controlled by the application of a magnetic nozzle. Thrust is transmitted to the device both from the reaction of the electrons with the magnetic field and the direct plasma reaction on the thrustor's physical structure. A detailed investigation of the exhaust beam has been carried out (reference 2). Local ion energies and fluxes were mapped by means of a Langmuir calorimetric probe, plasma potential surfaces were determined with an emitting probe, and electron temperature and density were measured with a Langmuir probe. Gross thrust measurements taken on a pendulum thrust stand agree favorably with the force calculated by integrating about a momentum contour in the exhaust beam. The presence of an ambipolar electric field was determined from the emitting probe survey. Its value is shown to be in agreement with that calculated from the measured electron pressure gradient. Calculation of the electron force on the magnetic field from electron pressure measurements and magnetic field shape indicates that about half the thrust is applied to the magnetic field.

REFERENCES

1. Seikel, G.R., Bowditch, D.N., and Domitz, S.: AIAA Papr 64-677, (August 1964).

2. Bowditch, D.N.: AIAA Paper 66-195, (March 1966).

A LANGMUIR CALORIMETRIC PROBE

TO DETERMINE AVERAGE ENERGY IN A PLASMA BEAM

By D. N. Bowditch

National Aeronautics and Space Administration
Lewis Research Center
Cleveland, Ohio

ABSTRACT

A plane guard-ringed Langmuir probe, Figure 1, is described that can simultaneously measure the current and power to the probe face. This is done by gluing a material which is both an electrical insulator and thermal resistance between the probe face and a water-cooled probe body. The thermal resistance is calibrated by determining the probe's dynamic response to step changes in heat input.

The characteristics of thermal power to the probe versus bias voltage is interpreted by use of collisionless sheath theory. If the probe is assumed to be in a plasma beam with average energy per ion of U_o (eV) and average ion velocity $v_o > \sqrt{\frac{kT_e}{m_{ion}}}$, the measured ion power flux to the probe surface is

$$P_{ion} = j_i U_o + j_i(\phi_i + \phi_w) + j_i(V_p - V) - j_s \phi_w \quad \text{for } V_p - V > 0$$

where j_i is the beam ion current density, ϕ_i is the ionization potential, ϕ_w is the surface work function, j_s is the probe secondary emission current density, and V and V_p are the probe potential and the plasma potential, respectively. In typical experiments the secondary emission current, j_s, is both essentially independent of bias voltage and small compared to the ion current, j_i. Thus, in the ion saturation region the slope of the probe power versus bias voltage determines the ion current. The difference between the directly measured current and the ion current yields the secondary emission current. With the aid of an independent measurement of plasma potential, V_p, typical probe characteristics such as Figure 2 can, therefore, be interpreted to obtain the average energy per ion in the plasma beam, U_o, and the ion current density,

j_i. Of particular interest in Figure 2 is that the energy flux of the ions in the plasma beam is only a fraction of the power received at the calorimeter at floating potential where in the past calorimetric measurements have generally been performed.

The probe described was used in Reference 1 to examine the exhaust of a plasma thrustor. Langmuir calorimetric probe and Langmuir probe measurements were combined to draw a momentum contour around the thrustor. To calculate the thrust the following assumptions were made:) all the ion energy, U_o , is directed energy, 2) the exhaust contains only singularly ionized ions, and 3) the exhaust has cylindrical symmetry. The thrust value thus calculated was only 18 per cent higher than the direct thrust stand measurement.

References

1. Bowditch, D. N., AIAA preprint 66-195, 1966.

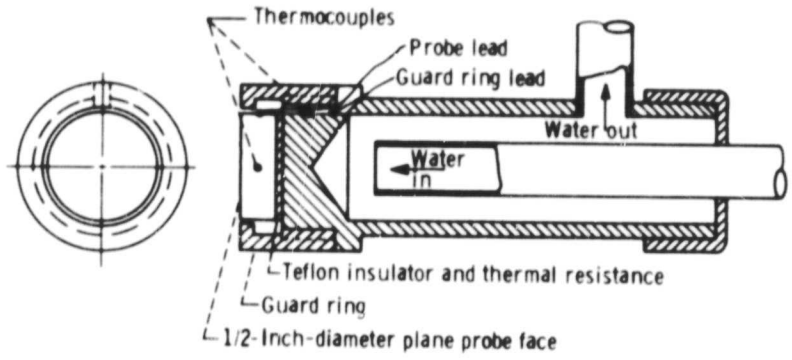

Figure 1 - Langmuir calorimetric probe

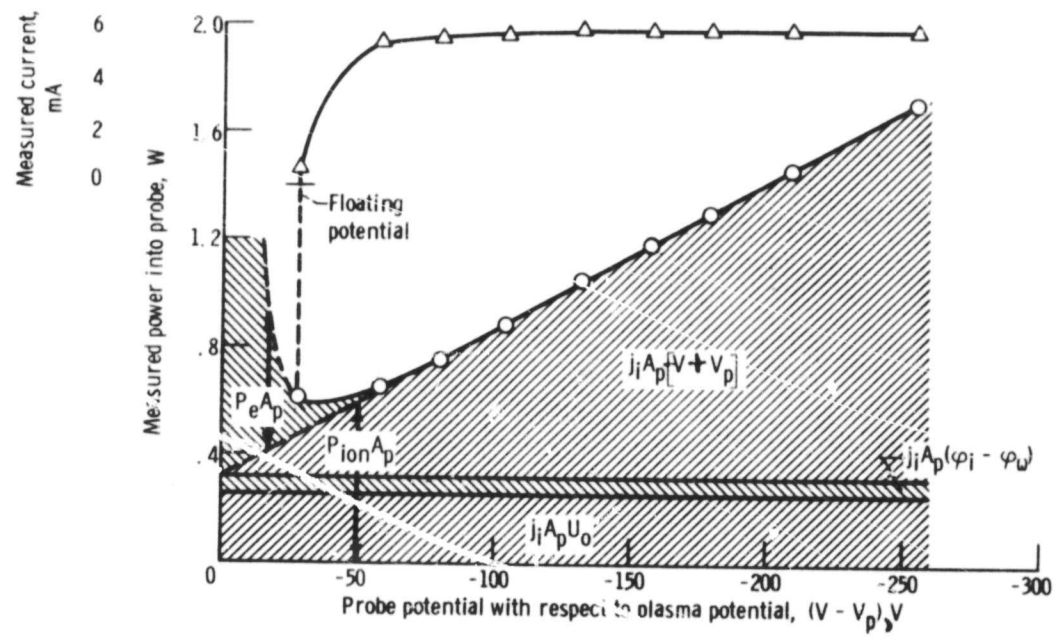

Figure 2 - Probe characteristics of power and current versus potential

RADIO FREQUENCY INDUCTION HEATING AND PRODUCTION OF PLASMAS AT LOW PRESSURE

By R. J. Sovie and G. R. Seikel

National Aeronautics and Space Administration
Lewis Research Center
Cleveland, Ohio

ABSTRACT

An experimental and theoretical investigation of radio frequency induction heating and production of plasma is described. The linearized analysis examines the coupling between a solenoidal radio frequency magnetic flux of peak strength B_o and a uniform cylindrical plasma of radius R. The general solution for the average power flux, $\overline{P}$, to the plasma is

$$\overline{P}\left[\frac{\text{WATTS}}{(\text{METER})^2}\right] = \frac{\omega\delta\left[1+(\omega\tau)^2\right]^{1/4}}{\sqrt{2}}\left(\frac{B_o^2}{2\mu_o}\right)\text{Real part of}\ \frac{J_1(\xi)}{J_0(\xi)}\ e^{-\frac{i}{2}\cot^{-1}\omega\tau}$$

(equation 1)
mks units

where $\omega/2\pi$ is the applied frequency, δ is the ordinary rf skin depth, τ is the electron momentum transfer collision time, and the normal Bessel functions, J_o and J_1, are functions of the complex dimensionless co-ordinate

$$\xi = \frac{R}{\delta}\left[\frac{-2i}{1+\omega\tau i}\right]^{1/2}$$

An important feature of this analysis is that the inertia terms are considered in the generalized Ohm's law. The effect of this term, which is of order $\omega\tau$ compared to the resistive term, is to permit deeper penetration of the applied field into the plasma.

The experiments have been conducted at the micron pressure level in helium with a 17.5 MH_z 2 Kw rf power supply. The 7.7 cm diameter 4-turn faraday shielded induction coil used to couple to the 4.8 cm diameter plasma discharge tube was designed to apply an approximately constant rf magnetic field over a length of 7.5 cm. In addition to detailed electrical circuit measurements, line ratio spectroscopy and microwave interferometry were used to measure the plasma electron temperature and density respectively. For all the experimental conditions investigated $\omega\tau > 3.5$, and the theoretical solution for the power flux to the plasma is well approximated by the limiting solution for $\omega\tau \gg 1$. For the experimental configuration investigated, the

total power coupled to the plasma, P, is

$$P(\text{watts}) = 3.94 \times 10^{-15} \sqrt{\rho} \, n_e \, I^2 \left[\frac{I_1^2(h)}{I_0^2(h)} - \frac{I_2(h)}{I_0(h)} \right]$$

(equation 2)
mks units

where $\sqrt{\rho}$ is the plasma resistivity, n_e is the electron density, I is the coil current, and the modified Bessel functions (I_0, I_1, and I_2) are functions of the dimensionless plasma radius, $h = \frac{\sqrt{2}R}{\delta\sqrt{\omega\tau}}$

The excellent comparison between the data obtained and equation 2 is illustrated in the accompanying figure. The theoretical and experimental investigation is being extended to determine the energy stored in the plasma and its effects on the impedance of the external circuit.

Figure 1 Comparison of Theoretical and Experimental Results for the Power Coupled To the PLASMA

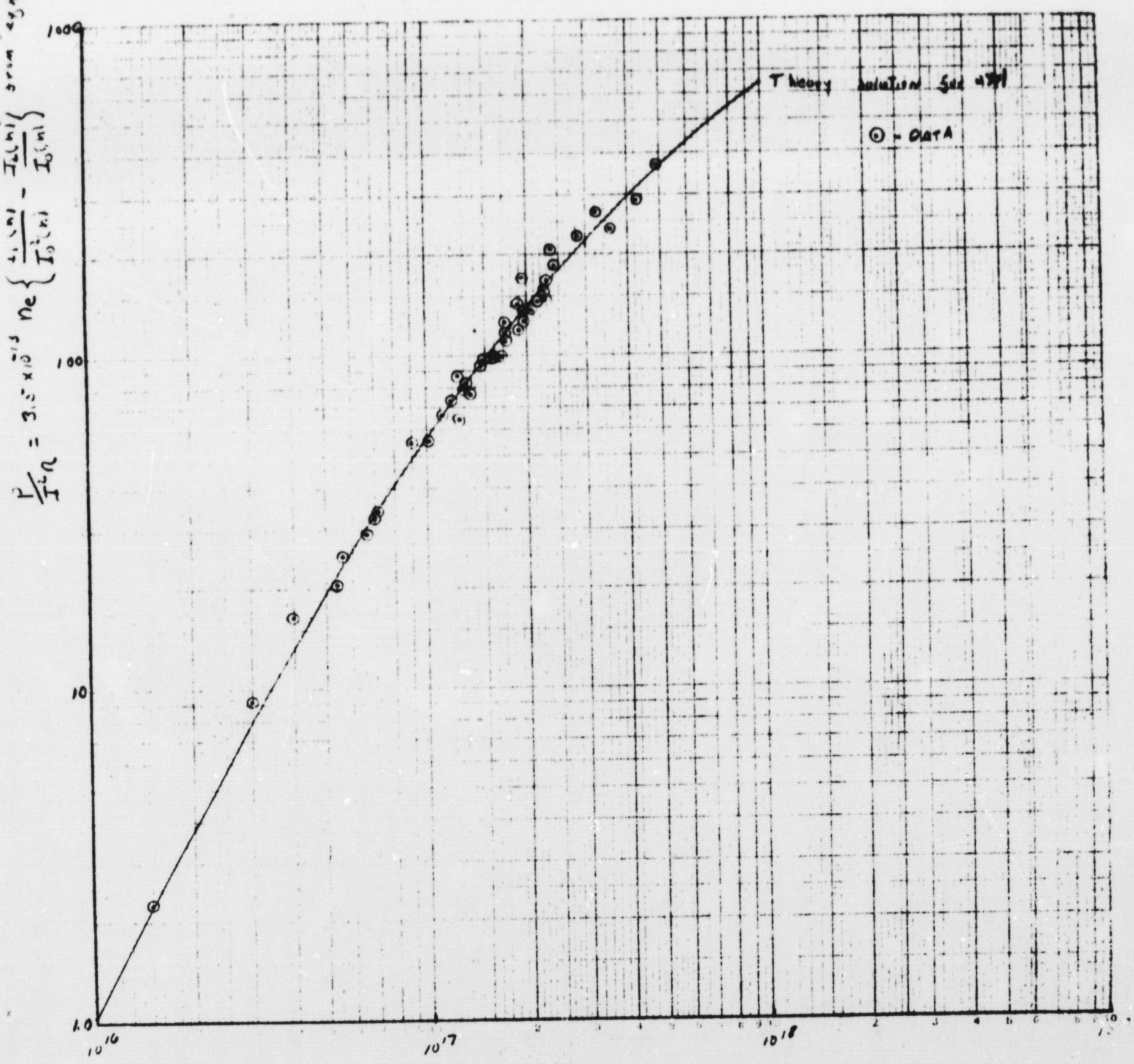

85-4/6

VOLUME ION PRODUCTION COSTS IN TENUOUS PLASMAS

By R. J. Sovie and J. V. Dugan, Jr.

National Aeronautics and Space Administration
Lewis Research Center
Cleveland, Ohio

ABSTRACT

The energy cost for ion production has been calculated for optically thin plasmas with a Maxwellian distribution of free electron energies by comparing the relative probabilities for the competing inelastic processes of excitation and ionization. Detailed results have been obtained for helium[1], argon[2], cesium and hydrogen[3] gases. Experimental excitation cross sections from the ground state have been used for the helium case. The semi-classical Gryzinski[4] method has been used to determine theoretically the cross-section needed for the argon and cesium calculations. It is generally considered that the Gryzinski method will give absolute cross-sections good to within a factor of two or better. However, using this method in an ev/ion calculation should not introduce an appreciable error since one is interested in the relative rates of the processes involved rather than the absolute magnitude of these rates. This method has also been used to calculate excitation and ionization cross-section for interaction between electrons and the metastable 2^1S and 2^3S states of helium. These cross-sections have been used to calculate the effects of electron-metastable atom interactions on the volume ion production processes in helium[5]. An approximate theory is also presented which gives the volume ion production cost for a general atom as a function of electron kinetic temperature. The results of this theory are compared with the results of the more detailed calculations for hydrogen, helium, argon and cesium.

REFERENCES

1. Sovie, R. J. and Klein, B. M. NASA TN D-2324, 1964.

2. Sovie, R. J. and Dugan, J. V., Jr. NASA TM X-52064, 1964.

3. Monnin, C. F. and Prok, G. M. To be published.

4. Gryzinski, M. Report N., PAN-448/XVIII, Inst. Nuclear Res., Polish Acad. Sci. (Warsaw) June 1963.

5. Sovie, R. J. and Dugan, J. V., Jr. NASA TN D-3121, 1965.

CHARGED PARTICLE TRANSPORT BY MONTE CARLO ANALYSIS

by C. M. Goldstein

ABSTRACT

The characteristics of one-dimensional electron diode with low pressure Argon scattering gas is analyzed by a Monte Carlo method. Experimentally determined differential elastic scattering cross-sections, extrapolated to zero energy, are employed. Current-voltage characteristics are compared with those obtained from a hard sphere collision model. Negative resistance is found for low emission current densities and low pressure as a result of the Ramsauer cross-section. The randomization of energy between velocity components is found to be quite large for accelerating potentials and pressure-electrode separation valves as low as 1/2 Torr-cm. The effect of non-isotropic scattering is not large for the diode conditions studied.

ELECTRON DISTRIBUTION FUNCTION AND NUMBER DENSITY IN NON-EQUILIBRIUM MHD PLASMAS

By Frederic A. Lyman, John V. Dugan, Jr. and Lynn U. Albers

National Aeronautics and Space Administration
Lewis Research Center
Cleveland, Ohio

ABSTRACT

The present work was undertaken to investigate the validity of local thermodynamic equilibrium (LTE) assumptions in the type of nonequilibrium discharge of interest for magnetohydrodynamic (MHD) power generation. The two-temperature LTE theory assumes that: (a) the free electron distribution function is maxwellian at a temperature T_e which may be considerably higher than the gas temperature, (b) the bound electron states are populated according to a Boltzmann distribution at T_e and (c) the free electron number density N_e has the Saha value corresponding to T_e.

The validity of assumptions (b) and (c) has been investigated by several workers (e.g., ref. 1). Assumption (a) has received less attention, however. It cannot be studied independently of the other two assumptions, because the rates of excitation and ionization depend strongly on the distribution function of the free electrons, which in turn is sensitive to any departure of the bound states from equilibrium. This paper reports preliminary results of an investigation undertaken to establish the validity of LTE for MHD plasmas. In general, the analysis involves numerical solution of the Boltzmann equation for the free electron energy distribution function $f(u)$ and the steady-state rate equations for the bound states. The problem was attacked in the following three stages.

First, $f(u)$ was calculated from a Boltzmann equation which included only the electric field and the elastic collision terms, N_e being obtained from the Saha equation. Typical results are shown in Fig. 1, where the theory is compared with the theory and experiment of Kerrebrock and Hoffman (ref. 2) on a graph of electrical conductivity versus current density for Ar + 0.15% K at 1 atm and 1500° K gas temperature. The main conclusion of these calculations was that the experimentally observed dip in the electrical conductivity at 10^3 amps - m^{-2} could not be explained by a non-maxwellian distribution function, as suggested by Kerrebrock and Hoffmann. Ref. 3 summarizes this phase of the work.

To investigate the effect of inelastic collisions on $f(u)$ and N_e, a five-level model cesium atom was chosen, consisting of three discrete excited states (6P, 5D, 7S) and a lumped state which encompasses all higher excited states. The characteristics of this

model atom were explored by solving the rate equations for the bound levels, assuming a maxwellian f(u). The results were in good agreement with previous work of BenDaniel and Tamor (ref. 1), despite significant differences in the excitation and ionization cross sections, and were relatively insensitive to changes in the binding energy and degeneracy of the lumped state. As expected, the escape probability for resonance radiation is the most important parameter in determining N_e and the state populations.

Finally, the simultaneous solution of the Boltzmann equation for f(u) (including all relevant elastic and inelastic collision terms) and the bound-state rate equations is being carried out numerically by an iterative technique. Typical results (ref. 4) are shown in Fig. 2 for Ar + 0.15% Cs at 1 atm pressure and 1500° gas temperature, for the case of complete trapping of resonance radiation (all other radiation is allowed to escape). The results show trends which are similar in some respects to Kerrebrock and Hoffman's data for Ar + K, but the conductivity decreases monotonically with decreasing current density, rather than increasing again below 10^3 amps - m^{-2} (this trend in experimental data is now believed to be due to residual ionization from the arc heater, see ref. 5).

Future plans are to improve convergence in the iterative solution, since some difficulty has been experienced when $T_e < 2300^{\circ}$ K (the dashed portion of the curve in Fig. 2), and to carry out calculations for a range of conditions of interest for MHD power generation. The investigation may also be extended to the analysis of other nonequilibrium plasmas.

REFERENCES

1. BenDaniel, D. J. and Tamor, S.: Nonequilibrium Ionization in Magnetohydrodynamic Generators. Rept. 62-RL-(2922-E), General Electric Research Lab., 1962.

2. Kerrebrock, J. L. and Hoffman, M. A.: Nonequilibrium Ionization Due to Electron Heating: II. Experiments. AIAA J. 2 (1964) 1080.

3. Lyman, F. A.: Maxwellization of Electrons in a Low-Voltage, Atmospheric Pressure Gas Discharge. AIAA J. (to be published).

4. Dugan, J. V., Jr., Lyman, F. A. and Albers, L. U.: Solution of the Boltzmann and Rate Equations for the Electron Distribution Function and State Populations in Nonequilibrium MHD Plasmas. Paper to be presented at International Symposium on Magneto-hydrodynamic Electrical Power Generation, Salzburg, Austria, July 4-8, 1966, (NASA TM X-52190).

5. Dethlefsen, R. and Kerrebrock, J. L.: Experimental Investigation of Fluctuations in a Nonequilibrium MHD Plasma. Proc. Seventh Symposium on Engineering Aspects of Magnetohydrodynamics, pp. 117-134.

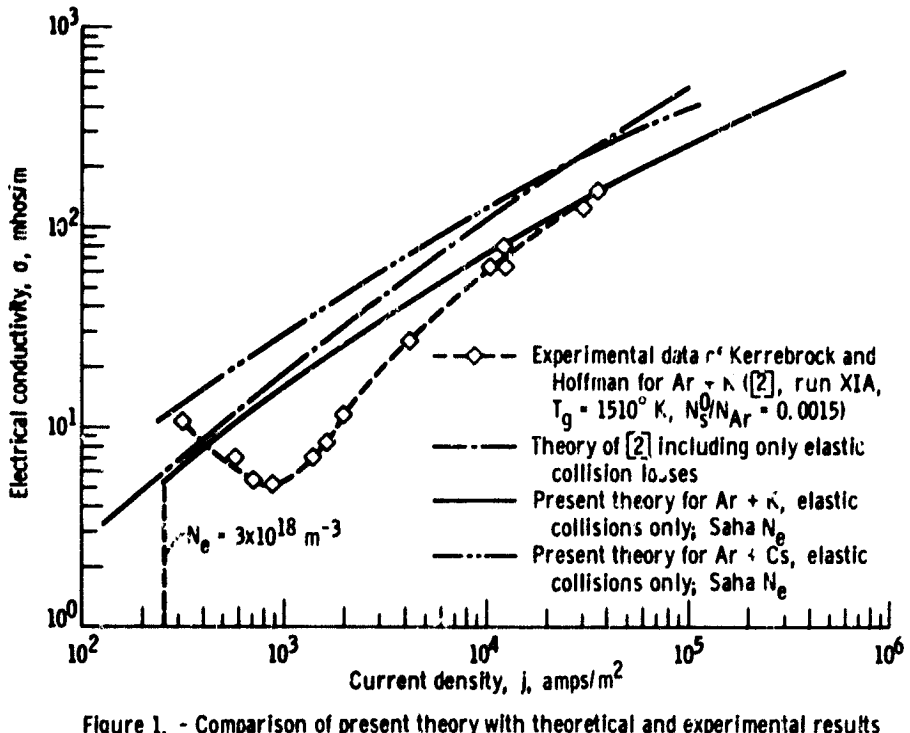

Figure 1. - Comparison of present theory with theoretical and experimental results of Kerrebrock and Hoffman [2]. Gas temperature, 1500° K; seed fraction, N_S^0/N_{Ar}, 0.0015.

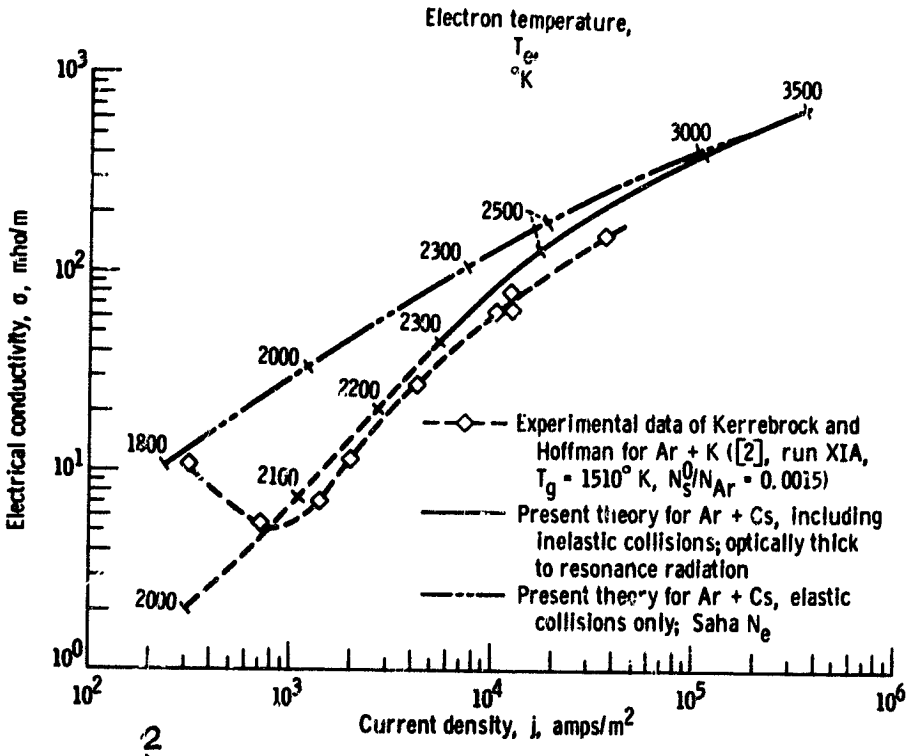

Figure 2. - Electrical conductivity as function of current density. Atmospheric pressure; gas temperature, 1500° K; seed fraction, 0.0015.

CALCULATION OF THREE-BODY COLLISIONAL RECOMBINATION COEFFICIENTS FOR CESIUM AND ARGON ATOMIC IONS WITH AN ASSESSMENT OF THE GRYZINSKI CROSS SECTIONS*

by John V. Dugan, Jr.

Lewis Research Center
National Aeronautics and Space Administration
Cleveland, Ohio

Argon seeded with cesium has been extensively studied as a promising system for MHD power generation using nonequilibrium plasmas.[1] Volume recombination coefficients α for carrier and seed ions are required for both the electron energy balance and the generalized Saha equations as was indicated in Ref. 2. The purpose of this study was to present theoretical results for these coefficients, compare them with experimental values, and point out the expected accuracy of the Gryzinski cross sections in the light of recent atomic beam results.

Collisional-radiative recombination coefficients have been obtained for pseudo-alkali and hydrogen atom plasmas by Bates et al[3] using a quasi-equilibrium, steady-state approximation. Byron et al[4] assumed in their hydrogen calculation that the limiting step in the chain of recombination events is deexcitation of bound electrons. The deexcitation rate is obtained from the excitation rate by the detailed balancing relation.[5] The recombination rate of Ref. 4 is simply the product of the minimum deexcitation rate and a factor β which accounts for nonequilibrium effects. The Gryzinski formulation[6] was employed in Refs. 3 and 4 to compute collision cross sections for excitation of bound electrons.

Byron, Bortz, and Russell[7] calculated recombination coefficients for atomic hydrogen, potassium, and argon for electron temperatures from 500° to 2000° K. They assumed that atomic energy levels form a "band" above and below each electronic quantum gap. Ref. 8 is a calculation of the purely collisional α for cesium via the Byron method[4] but with detailed consideration of the discrete electronic states. The Gryzinski excitation cross sections were used to calculate transitions between these states. The range of electron temperatures T_e studied was extended to include 500° to 10,000° K, values of interest for the MHD generator utilizing nonequilibrium conductivity.[1]

The three-body coefficient α_{rec} from several sources is plotted versus T_e in Fig. 1. For the curve from Ref. 8, the quantum gaps which correspond to the minimum deexcitation rates are indicated. The dashed curve gives the results of Ref. 7 for potassium, while the

*Submitted to Journal of Applied Physics as Communication

broken curves from Ref. 3 are for a pseudo-alkali atom plasma. The coefficient from Ref. 3 is a function of number density N_e because radiative deexcitation and two-body capture are included. The results are in good agreement with those of Ref. 9 performed for a 26 level model atom including all collisional and radiation effects.

The agreement between theory and experiment[10,11,12] for the alkali first and total excitation cross sections is well within the expected accuracy of the slope of the Gryzinski values[3,8] near threshold (the critical region for low electron temperatures). The first excitation cross section (cm^2) for cesium is low by a factor of 3 at peak[13,14]; but in the near threshold region, the Gryzinski slope, 30 $Å^2 eV^{-1}$, is about one-half of the experimental value, 75 $Å^2 eV^{-1}$, for the first one eV. The (Maxwell averaged) Gryzinski total excitation coefficients, however, are as small as one-sixth of experiment[15] for T_e values from 1000 to 3000° K. Also, radiation effects may be important in both recombination experiments and MHD systems. The contribution of this deexcitation mechanism depends on the superelastic collision rate and optical absorption cross section of the important ionizing species.[2,7,8]

Values of α'_{rec} for argon were calculated in the same fashion as the cesium coefficients and are plotted versus T_e in Fig. 2 and compared with the hydrogen results of Refs. 3 and 7. The neglect of radiative deexcitation in the collisional calculation becomes less important at high temperatures as was pointed out in Ref. 8 where the mean radiative transition probabilities were compared with the superelastic collision frequencies.[8] In part it has been shown that the purely collisional approach is a good approximation for cesium, even down to $10^{13} cm^{-3}$ [8,9], while the maximum radiative correction for argon is estimated to be 50 percent at T_e = 10,000° K. However, the absorption cross section for the argon resonance line may be relatively small which would lead to considerable energy loss by line radiation.

As regards seeding criteria for nonequilibrium MHD power generation, recombination rates will not be very different for carrier and seed gases at achievable electron temperatures.[1] However, the average energy lost by the free electrons in recombination will depend on the mechanism by which the captured electrons become deexcited.

REFERENCES

1. J. E. Heighway, and L. D. Nichols: NASA TN D-2651, Feb. 1965.

2. T. Hiramoto: J. Phys. Soc. Japan 20, June 1965, p. 1061.

3. D. R. Bates, A. E. Kingston, and R. W. P. McWhirter: Proc. Roy. Soc. London, A-267, May 1962, p. 297.

4. S. Byron, R. C. Stabler, and P. I. Bortz: Phys. Rev. Lett., 8, no. 9, May 1962, p. 376.

5. R. H. Fowler: Statistical Mechanics. 2nd ed., Ch. XVII, Cambrid Univ. Press, 1936.

6. M. Gryzinski: Phys. Rev. I, II, III 138, no. 2A, April 1965, p.

7. S. Byron, P. Bortz, and G. Russell: Proc. of 4th Symp. on Eng. Aspects of MHD, Univ. of Calif., April 10-11, 1963.

8. J. V. Dugan, Jr.: NASA TN D-2004, Oct. 1964.

9. D. W. Norcross, and P. M. Stone: Sperry Rand RR-66-31, April 1966.

10. J. Y. Wada, and R. C. Knechtli: Phys. Rev. Lett., 10, no. 12, June 1963, p. 513.

11. Yu. M. Aleskovskii: Soviet Phys.-JETP, 17, no. 13, Sept. 1963, p. 570.

12. L. P. Harris: Rep. 64-RL-3698G, Gen. Elec. Co., June 1964.

13. J. W. Sheldon, and J. V. Dugan, Jr.: J. App. Phys., 36, no. 2, Feb. 1965, p. 650.

14. I. P. Zapesochny, and L. L. Shimon: Abstracts of IVth Internat'l Conf. on the Phys. of Electronic and Atomic Collisions, Laval Univ., Quebec City, Canada, Aug. 2-6, 1965, p. 401.

15. J. F. Nolan: Summary Report for NASA, CR-54670, Jan. 1966.

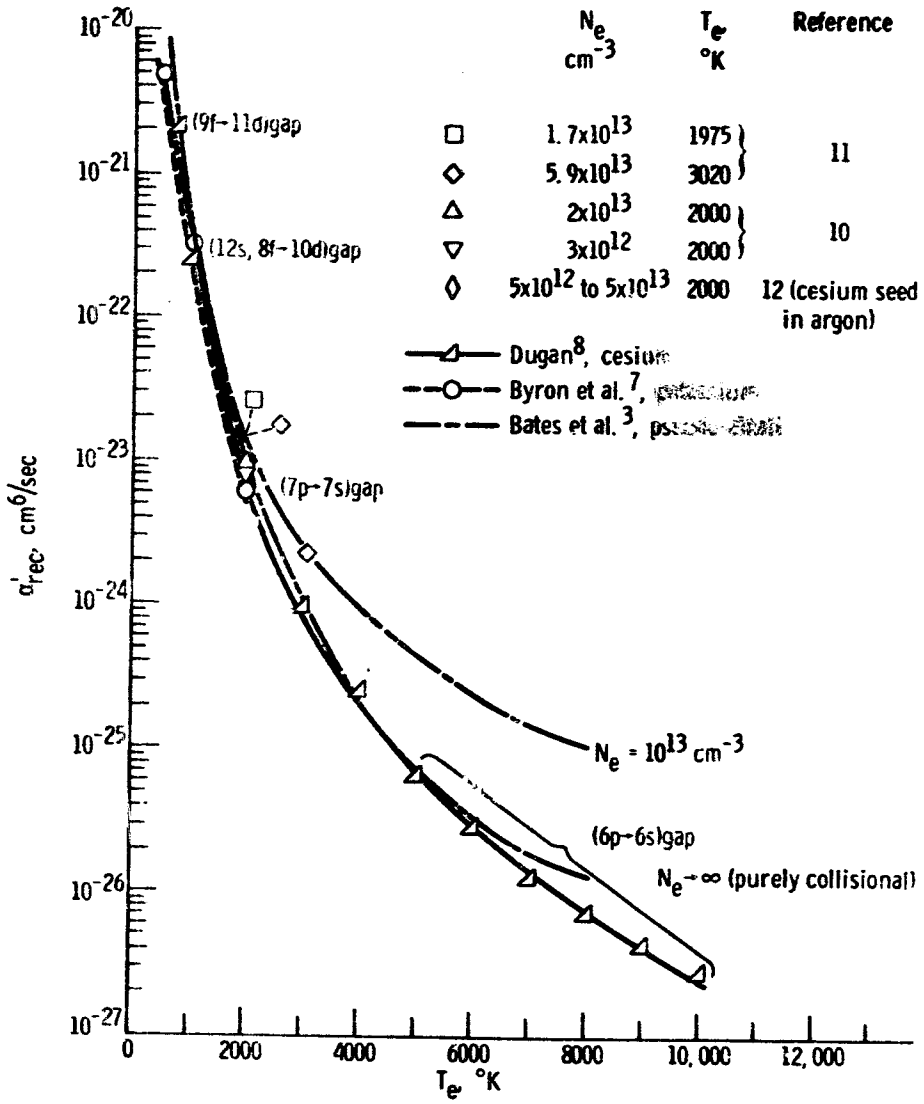

Figure 1. - Alkali three-body collisional recombination coefficients as function of free-electron temperature for range of electron number density (10^{13} to 10^{18} cm^{-3}).

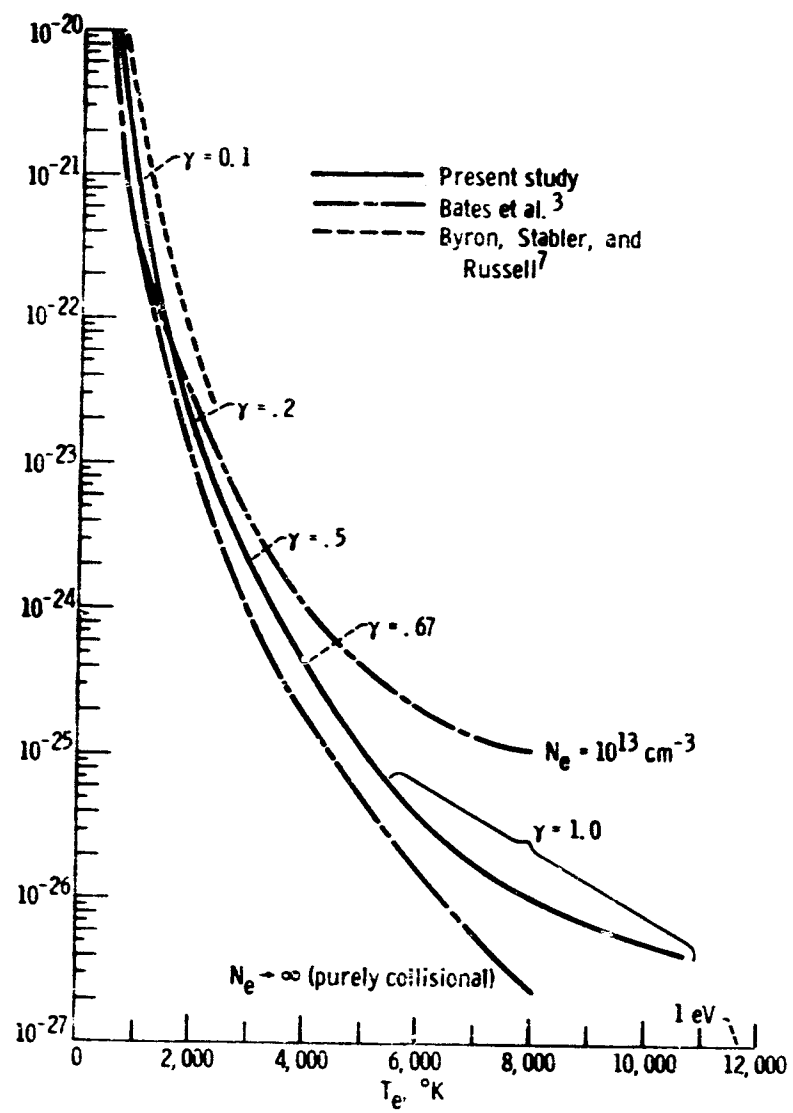

Figure 2. - Argon and hydrogen three-body collisional recombination coefficients as functions of electron temperature for range of electron number density (10^{13} to 10^{18} cm^{-3}).